Journal of Physiology (1991), **440**, *pp.* 735–769
With 14 *figures*
Printed in Great Britain

A FUNCTIONAL MICROCIRCUIT FOR CAT VISUAL CORTEX

BY RODNEY J. DOUGLAS*† AND KEVAN A. C. MARTIN*

*From the *MRC Anatomical Neuropharmacology Unit, Department of Pharmacology, South Parks Road, Oxford OX1 3QT and the †Department of Physiology, University of Cape Town Medical School, Observatory 7925, Cape Town, South Africa*

(*Received 6 March 1990*)

SUMMARY

1. We have studied *in vivo* the intracellular responses of neurones in cat visual cortex to electrical pulse stimulation of the cortical afferents and have developed a microcircuit that simulates much of the experimental data.

2. Inhibition and excitation are not separable events, because individual neurones are embedded in microcircuits that contribute strong population effects. Synchronous electrical activation of the cortex inevitably set in motion a sequence of excitation and inhibition in every neurone we recorded. The temporal form of this response depends on the cortical layer in which the neurone is located. Superficial layer (layers 2+3) pyramidal neurones show a more marked polysynaptic excitatory phase than the pyramids of the deep layers (layers 5+6).

3. Excitatory effects on pyramidal neurones, particularly the superficial layer pyramids, are in general not due to monosynaptic input from thalamus, but polysynaptic input from cortical pyramids. Since the thalamic input is transient it does not provide the major, sustained excitation arriving at any cortical neurone. Instead the intracortical excitatory connections provide the major component of the excitation.

4. The polysynaptic excitatory response would be sustained well after the stimulus, were it not for the suppressive effect of intracortical inhibition induced by the pulse stimulation.

5. Intracellular recording combined with ionophoresis of γ-aminobutyric acid (GABA) agonists and antagonists showed that intracortical inhibition is mediated by $GABA_A$ and $GABA_B$ receptors. The $GABA_A$ component occurs in the early phase of the impulse response. It is reflected in the strong hyperpolarization that follows the excitatory response and lasts about 50 ms. The $GABA_B$ component occurs in the late phase of the response, and is reflected in a sustained hyperpolarization that lasts some 200–300 ms. Both components are seen in all cortical pyramidal neurones. However, the $GABA_A$ component appears more powerful in deep layer pyramids than superficial layer pyramids.

6. The microcircuit simulates with good fidelity the above data from experiments *in vivo* and provides a novel explanation for the apparent lack of significant inhibition during visual stimulation. The basic circuit may be common to all cortical areas studied and thus the microcircuit may be a 'canonical' microcircuit for neocortex.

MS 8328

INTRODUCTION

We have studied the intracellular responses of cortical neurones to visual stimulation and have analysed the possible inhibitory mechanisms involved in cortical processing (Berman, Douglas, Martin & Whitteridge, 1991; Douglas, Martin & Whitteridge, 1991). In the course of these investigations we encountered a general puzzle which is best illustrated with the example of direction-selective neurones in visual cortex. Many of these directionally selective neurones receive monosynaptic excitation from neurones of the lateral geniculate nucleus. However, geniculate neurones have circularly symmetric receptive fields and respond equally well to motion in all directions (Hubel & Wiesel, 1959). Thus the direction selectivity in cortical neurones is generated postsynaptically from a non-directional excitatory input.

The mechanisms thought to underlie directionality have been studied for at least two decades, using extracellular recording techniques. The answer that has emerged is that cortical direction selectivity arises because postsynaptic inhibitory processes quench the strong excitation arriving from the lateral geniculate neurones when the stimulus moves in the non-preferred direction (Bishop, Coombs & Henry, 1971; Goodwin & Henry, 1975; Goodwin, Henry & Bishop, 1975; Bishop, Kato & Orban, 1980; Ganz & Felder, 1984; see Orban, 1984). The puzzle is that our intracellular recordings revealed little of the anticipated inhibition: there was little or no hyperpolarization of the membrane (Douglas *et al.* 1991), and no evidence of significant shunting inhibition when the stimulus was moved in the non-preferred direction (Berman *et al.* 1991). Indeed, similar results were obtained for orientation and subfield antagonism in simple cells (Douglas, Martin & Whitteridge, 1988; Berman *et al.* 1991; Douglas *et al.* 1991).

One possible explanation of our results is that the inhibitory synapses were some distance from the soma and their actions were masked by the impedance of the intervening dendrites. The dendritic spines are particularly relevant here because their electrical properties may make them relatively isolated from the dendritic trunks. Individual geniculocortical synapses, which are frequently located on spines, could be subject to a 'synaptic veto' operation if the inhibitory synapse were placed on the same spine (Diamond, Gray & Yasargil, 1970; Koch & Poggio, 1983, 1985*a*). In exploring this possibility, however, we found that most spines receiving an identified geniculate afferent synapse do not receive an additional putative inhibitory synapse (Dehay, Douglas, Martin & Nelson, 1991). Most putative inhibitory synapses are not on spines, but on proximal dendritic shafts (Beaulieu & Somogyi, 1990; see Martin, 1988; White, 1989), which are probably electrotonically close to the soma and thus should be visible in intracellular recording (Douglas & Martin, 1990; Koch, Douglas & Wehmeier, 1990). We are left with a conundrum: the *appearance* of strong inhibition in extracellular recordings in the face of intracellular evidence against strong inhibition.

In an effort to understand how the cortical circuits perform their effortless and near-invisible shaping of cortical excitation, we explored the cortical inhibitory processes using electrical stimulation rather than visual stimulation. It has long been known that inhibitory postsynaptic potentials (IPSPs) can be evoked consistently in neurones of the visual cortex by stimulating either the thalamic afferents (Li, Ortiz-

Galvin, Chou & Howard, 1960; Watanabe, Konishi & Creutzfeldt, 1966; Toyama, Matsunami & Ohno, 1969), or by direct stimulation of the cortical surface (Li & Chou, 1962; Dreifuss, Kelly & Krnjević, 1969). By using electrical pulse stimuli together with conventional methods of ionophoresis of drugs, we hoped to learn more about the nature of the cortical IPSPs and so gain some insight to the action of inhibition during natural stimulation.

Since the neurones we were studying form part of a network of highly interconnected neurones, we used a microcircuit whose operation could be simulated on a computer to aid us in the interpretation of our data. The microcircuit was built up from elemental components of the cortical circuits, based on our previous microanatomical, immunocytochemical, and electrophysiological studies (reviewed in Martin, 1984; Martin, 1988; Somogyi, 1989). We compared the performance of the microcircuit with the experimental data obtained using the simple pulse stimulus. Although the pulse stimulus is artificial and the microcircuits are reduced to the minimum of components in the model, such simplification provided a means of interpreting the pulse responses, and offered an interesting solution to the conundrum posed above. A preliminary report of an earlier version of the microcircuit has been published (Douglas, Martin & Whitteridge, 1989).

METHODS

Our methods are described in Douglas *et al.* (1991). Briefly, neurones were recorded from the postlateral gyrus of the striate visual cortex (area 17) of twelve anaesthetized, paralysed cats (Martin & Whitteridge, 1984; Douglas *et al.* 1988), while continuously monitoring vital signs. Glass micropipettes were filled with 2 M-potassium citrate, or a 4% buffered solution of horseradish peroxidase (HRP) in 0·2 M-KCl. 8-Aminobutyric acid (GABA) agonists and antagonists were applied ionophoretically via a multibarrelled pipette using a Neurophore (Medical Systems Inc.). The concentrations used were as follows: GABA, 0·5 M; *n-m*-bicuculline, 0·01–0·1 M; baclofen, 0·01–0·1 M. The intracellular electrode was mounted in a 'piggy-back' configuration on a multibarrelled ionophoretic pipette. The tip of the recording electrode was separated from the tips of the ionophoretic barrels by 20–30 μm. The tip diameter of the ionophoretic pipette was about 5 μm, with impedances of 10–50 MΩ per barrel. Ejection currents for GABA ranged from 10 to 60 nA, for *n-m*-bicuculline from 20 to 200 nA, and for baclofen from 50 to 80 nA.

The receptive fields of the cortical neurones were first plotted in detail by hand, and then intracellular recordings were made via a Neurolog NL102 amplifier (Digitimer) and the data logged on a CED1401 (Cambridge Electronic Design). Where possible, HRP was injected intracellularly following data collection, to permit morphological identification of the recorded neurones.

Individual cortical neurones are embedded in a cortical microcircuit and their response to afferent stimulation cannot be tested in isolation. One of the simplest external stimuli that can be applied to the cortical network is an electrical impulse stimulation of the geniculocortical afferent fibres (Hoffman & Stone, 1971; Bullier & Henry, 1979; Henry, Harvey & Lund, 1979; Martin & Whitteridge, 1984). The contamination due to activation of corticofugal fibres appears to be small (Bullier & Henry, 1979; Ferster & Lindström, 1983; Martin & Whitteridge, 1984).

Although electrical stimulation is unnatural because it induces a highly synchronous and abnormally patterned activation of afferents, its value in analysing synaptic circuitry is well proven (Eccles, 1964). In the context of this study it offers a number of advantages. The stimulus is easily controlled, and highly reproducible. Direct activation of the cortical afferents reduces the contribution of retinal and thalamic processing in the cortical response and so is applicable to any cortical area, in particular the many cortical areas whose natural stimulus requirements are not yet known. Pulse stimulation (which need not be electrical) is also a popular engineering test signal because it offers many mathematical advantages in the analysis of systems (see Jack, Noble & Tsien, 1975).

RESULTS

Physiological responses

Intracellular recordings were made from 102 neurones in area 17 from all layers except layer 1. Their intracellular responses to electrical stimulation of the lateral

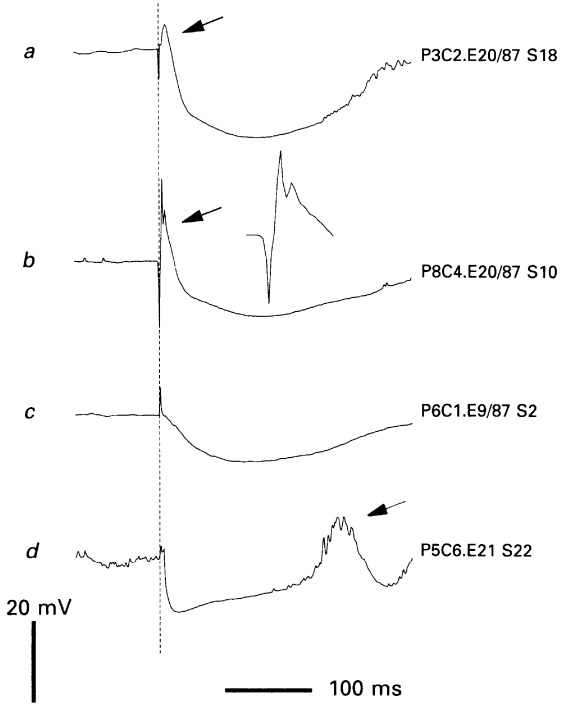

Fig. 1. Responses of cortical neurones to electrical stimulation of the geniculocortical afferents. In this and following figures, the dashed vertical line indicates the stimulus onset (0·2–0·4 ms, 200–400 μA), and every fourth point of the intracellular records has been plotted. *a*, response of layer 2+3 neurone to stimulation from electrodes at position OR2. An early depolarization (arrowed), lasting about 15 ms, was followed by a strong hyperpolarization which reached a maximum of −20 mV (with respect to control) after about 100 ms. *b*, response of layer 2+3 neurone stimulation at OR2. The arrowed initial depolarization is shown magnified in time. The stimulus artifact is large but is followed by a clear long-duration hyperpolarization. *c*, response of layer 2+3 neurone to stimulation at OR2. In this instance there was no clear initial depolarization, only the long-lasting hyperpolarization. *d*, response of layer 5+6 neurone to stimulation from OR2. A small depolarization is followed by a rapid onset hyperpolarization and an excitatory rebound (arrowed), which in turn was followed by a second hyperpolarization.

geniculate afferents from electrodes placed immediately above the lateral geniculate nucleus (site OR1) or in the cortical white matter (site OR2) were examined in 827 averaged records. The same general pattern of response (Fig. 1) was seen in all records: a short lasting (5–30 ms) depolarizing potential (the compound excitatory postsynaptic potential (EPSP), arrowed in Fig 1 *a* and *b*; shown enlarged for inset in *b*) followed by a long-lasting (100–300 ms) hyperpolarizing response (the IPSP). In no case did we observe an EPSP without an accompanying IPSP.

Action potentials were sometimes present during the control and the response

period. Since most action potentials were not synchronized with the stimulus (with the exception of some mono- or disynaptic responses in the early post-stimulus region), their amplitudes are greatly attenuated by the averaging procedure.

In some cases the IPSP was followed by an excitatory rebound (arrowed in Fig. 1*d*) and a further hyperpolarization. Some of the range of variation in the general pattern of response is illustrated in Fig. 1. This variation was perhaps not unexpected given that we were recording from different types of neurones in different layers of the cortex.

Laminar organization of the response pattern

Although the pattern of response of the actual cortical neurones did vary considerably, further analysis revealed two distinct patterns of response (Fig. 2). The illustrated patterns are from one spiny stellate and twenty-eight pyramidal neurones in the sample that were morphologically identified by intracellular injection of horseradish peroxidase (HRP). The first group was characterized by a very short latency (< 6 ms) EPSP followed by a rapid onset of the IPSP (mean latency 31 ms to maximum hyperpolarization; Fig. 2, right column). The second group was characterized by a longer EPSP (2–3 times longer), and a much slower evolution of the IPSP (mean latency 111 ms to maximum hyperpolarization; Fig. 2; left column). These two groups were not correlated with receptive field type or ordinal position (e.g. mono- or disynaptic activation by thalamic afferents). Instead they were strongly correlated with the cortical layer in which they were found (Fig. 3). In the sample of twenty-eight pyramidal neurones labelled with HRP the first response type was found exclusively in neurones of layer 5+6, while the second type was restricted to layers 2+3. The response of the spiny stellate cell (layer 4) was similar to that of the superficial pyramids. Most surprisingly the response of the layer 5 pyramidal neurones were not distinguishable from those of the layer 6 pyramidal neurones, nor layer 2 from layer 3 pyramidal neurones.

This finding of differences between the superficial and deep layers suggested that there might be two entirely separate circuits for the pyramidal neurones, one for superficial layers, and another for deep layers. However, the anatomy argued against assuming such an arrangement, because of the rich interconnections between the layers (Gilbert & Wiesel, 1979; Somogyi, Kisvárday, Martin & Whitteridge, 1983; Martin & Whitteridge, 1984; Kisvárday, Martin, Friedlander & Somogyi, 1987). Thus, we assumed that the difference was somehow contained in a single cortical circuit that connected layers 5+6 with layers 2+3.

Possible circuits underlying the pulse response

In order to identify the neuronal elements that might underlie this response, we attempted to simulate the response using a pulse input to idealized neurones, described in the Appendix. In this section we show the stages of development of a microcircuit that provides a remarkably accurate simulation of the experimental data.

We began with the simplest possible combination: afferent fibres exciting cortical neurones (Fig. 4*A*). This is a combination frequently used in models of cortical circuits, for example in the simple cell model of Hubel & Wiesel (1962), which has recently been formalized in a computer model to show how orientation tuning in

simple cells might be created (Ferster, 1988). The trace shows the simulated intracellular response to a pulse input to a model neurone 'recorded' intracellularly as the left-hand schematic shows. The right-hand schematic is a block diagram, which summarizes the left circuit. The block represents the average properties of a

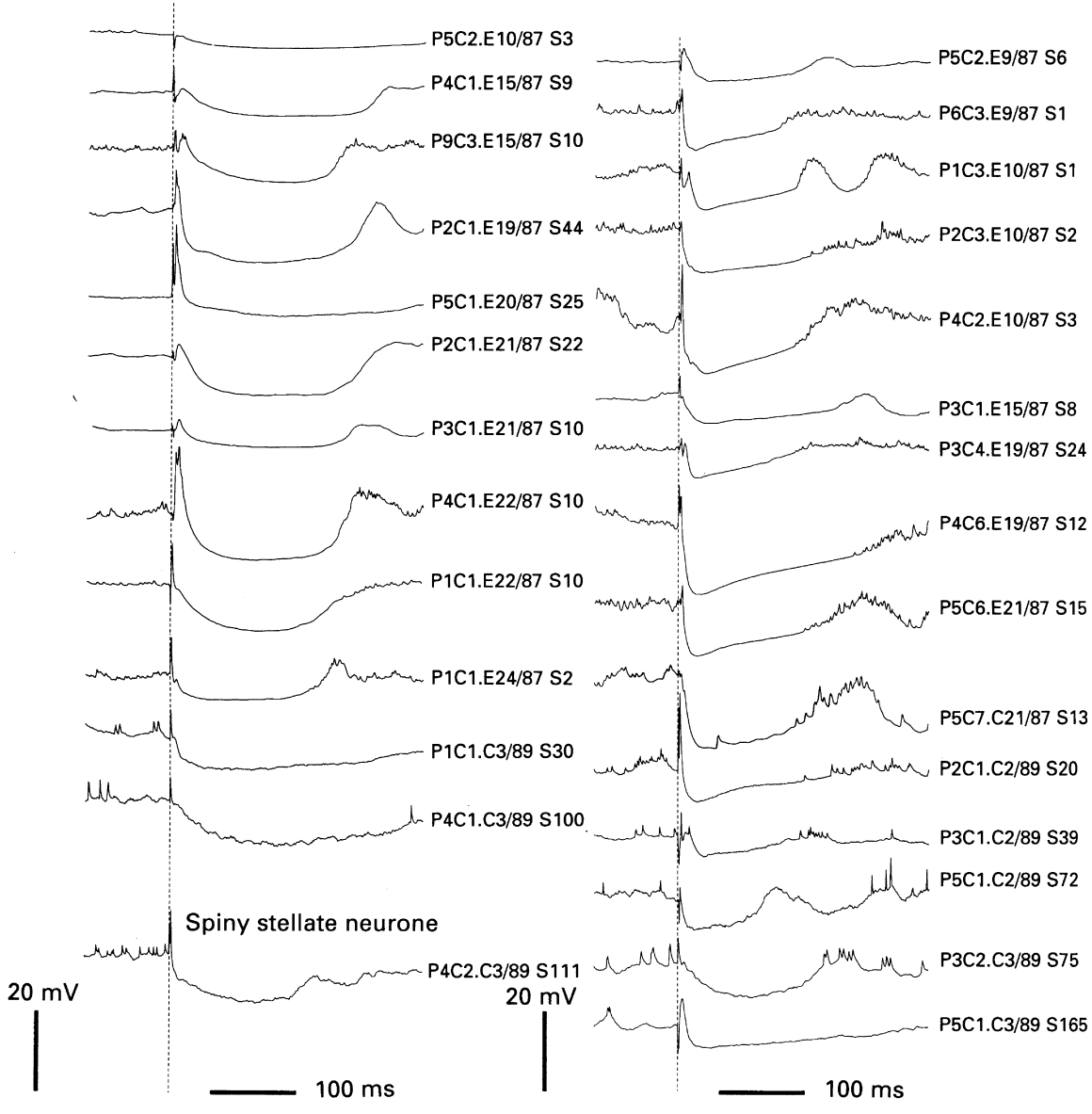

Fig. 2. Averaged responses ($n = 6$–30) of morphologically identified spiny neurones to electrical stimulation of afferents. Column on left shows responses of pyramidal neurones located in layers 2+3, and one spiny stellate neurone in layer 4. Right-hand column shows response for neurones in layers 5+6. Note that layer 2+3 neurones tend to have more prominent EPSPs and more slowly developing IPSPs than neurones in layer 5+6.

subpopulation of neurones. For this circuit the membrane potential only depolarized, producing an EPSP. Thus, the model 'intracellular' response does not resemble the response we recorded in actual cortical neurones.

In the cortex, spiny neurones, which are excitatory, are highly interconnected; 80–90% of pyramidal cell synapses are onto other spiny neurones, probably other

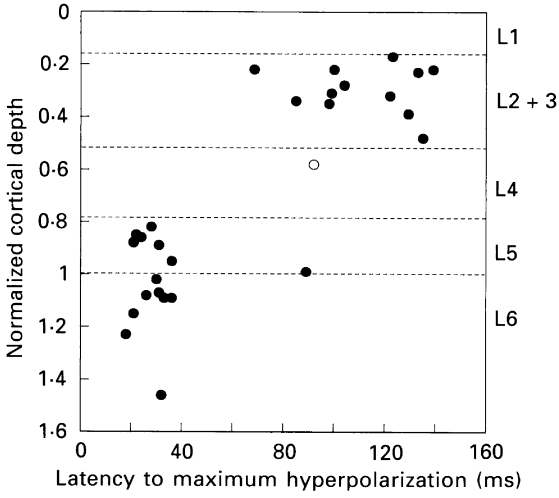

Fig. 3. Laminar differences in the evolution of hyperpolarizing IPSPs for morphologically identified spiny neurones. ●, normalized laminar (L1–L6) location of the soma. The depths of somata and laminar boundaries were expressed as a fraction of the depth of the layer 5/6 border. Pyramidal neurones in deep layers hyperpolarize rapidly (about 30 ms) to their maximum value, while pyramidal neurones of superficial layers take considerably longer (80–140 ms) to reach maximum hyperpolarization. Spiny stellate neurone of layer 4 (○) lies within superficial layer pyramid range.

pyramidal neurones (Kisvárday, Martin, Freund, Maglocsky, Whitteridge & Somogyi, 1986; Gabbott, Martin & Whitteridge, 1987; Somogyi, 1989; see White, 1989). These intracortical connections would therefore add to the initial excitation produced by the geniculate afferents. The schematic diagrams (Fig. 4*B*) show such a circuit and its summary block diagram. The trace shows the response of the model neurone, which depolarized considerably more for the same afferent input shown in Fig. 4*A*. The response shows quite clearly the two stages of excitation: the monosynaptic thalamic component and disynaptic cortical component. The significance of this will be discussed further below. The continued re-excitation by the cortical interconnections ensures that the neurone stays depolarized, unlike the condition shown in Fig. 4*A*.

Clearly the simulated responses shown in Fig. 4*A* and *B* differ significantly from the actual responses shown in Figs 1 and 2, which are dominated by the long-lasting hyperpolarizing IPSP. Thus, inhibitory neurones need to be included in the circuit. In the visual cortex, inhibition is thought to be mediated by the smooth neurones, particularly the basket cells, which make most (80–90%) of their synapses on spiny neurones, i.e. pyramidal and spiny stellate cells (Martin, Somogyi & Whitteridge, 1983; Somogyi *et al.* 1983; Somogyi & Soltész, 1986; Gabbott *et al.* 1987; Kisvárday *et al.* 1987; Somogyi, 1989). Figure 4*C* shows a more complex circuit where inhibitory

neurones were embedded in a circuit of excitatory neurones. The simulated response of such a circuit now more closely resembles the actual response seen in cortical neurones (Figs 1 and 2). The final step was to link two such circuits together to explore the source of the difference in response between the superficial and the deep layers.

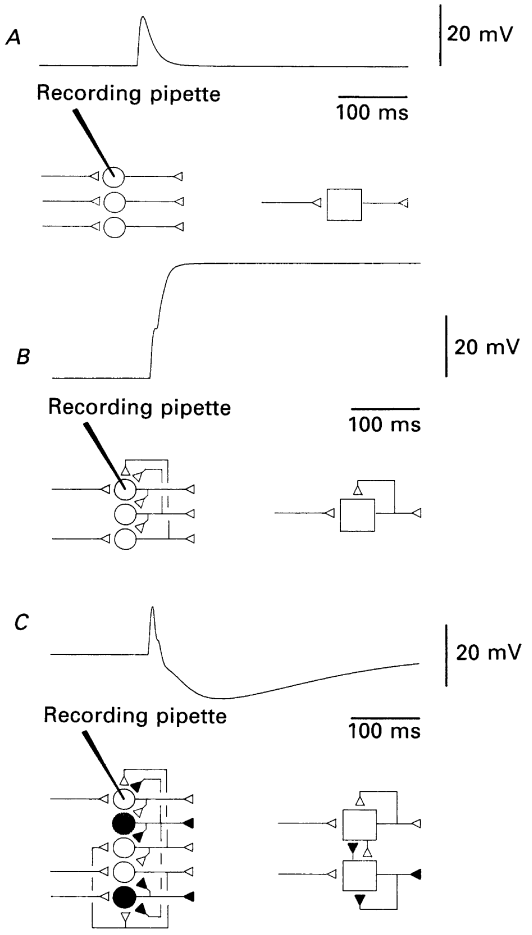

Fig. 4. Stages of development of model. *A*, first stage. Cortical afferents activating neurones are shown in left-hand schematic diagram and summarized in block diagram on right. The top trace shows the simulated response to a pulse input recorded 'intracellularly' in one neurone. *B*, second stage. Circuit from first stage modified to include excitatory interconnections between cortical neurones. Summary block diagram shown on right. Trace shows simulated response to a single pulse input. *C*, third stage. 'Inhibitory' neurones (filled symbols) are now embedded in excitatory circuit. Summary schematic diagram on right. $GABA_A$ and $GABA_B$ receptor responses are both simulated. Trace now shows biphasic EPSP–IPSP sequence similar to that seen in actual cortical neurones.

The structure of the microcircuit

The connections between the laminae were obtained from the literature describing the intracortical projections of HRP-labelled neurones (Gilbert & Wiesel, 1979; Freund, Martin, Smith, Somogyi, 1983; Somogyi *et al.* 1983; Martin & Whitteridge,

1984; Martin & Somogyi, 1985; Kisvárday *et al.* 1986; Gabbott *et al.* 1987; Martin, 1988; Somogyi, 1989). Briefly, spiny neurones in layers 2, 3 and 4 have their principle connections to those layers, but also send projections to layer 5. Spiny neurones in layers 5 and 6 have connections within both these layers, and ascending projections to layers 2, 3 and 4.

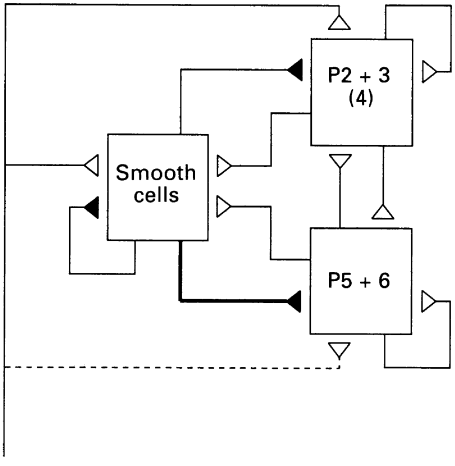

Fig. 5. Block diagram of circuit that successfully models the intracellular responses of cortical neurones to stimulation of thalamic afferents. Three populations of neurones interact with one another: one population is inhibitory (smooth cells, filled synapses), and two are excitatory (open synapses), representing superficial (P2+3) and deep (P5+6) layer pyramidal neurones. The layer 4 spiny stellate cells (4) are incorporated with the superficial group of pyramidal cells. Some neurones within each population receive excitatory input from the thalamus. Continuous *versus* dashed lines indicate that thalamic drive to the superficial group is stronger. The inhibitory inputs activate both $GABA_A$ and $GABA_B$ receptors on pyramidal cells. The thick continuous line connecting smooth cells to P5+6 indicate that the inhibitory input to the deep pyramidal population is relatively greater than that to the superficial population. However, the increased inhibition is due to enhanced $GABA_A$ drive only. The $GABA_B$ inputs to P5+6 are similar to those applied to P2+3.

A characteristic of smooth neurones is that they connect to targets in both superficial and deep layers, for example, layer 3 basket cells make synapses on pyramidal neurones in superficial and deep layers (Somogyi *et al.* 1983). Similarly, basket cells in layer 5 make synapses on pyramidal neurones in the deep layer and the superficial layers (Kisvárday *et al.* 1987; summarized in Somogyi & Martin, 1985; Somogyi & Soltész, 1986). Similar patterns are seen for other inhibitory cell types (Martin, 1984, 1988; Somogyi & Martin, 1985; Somogyi, 1989). Thus, for the present purposes we regard the smooth neurones as a single group within the cortical circuit.

The connections are summarized in the block diagram of Fig. 5. The spiny neurones (stellates and star pyramids) of layer 4 and grouped together with the superficial pyramids because their main connections appear to be with the superficial layers (Gilbert & Wiesel, 1979; Martin & Whitteridge, 1984). The single spiny stellate cell we recovered had a stimulus-evoked pattern resembling that of the superficial

pyramids (Fig. 2). The smooth cells were not differentiated into separate groups because we did not recover any we might have recorded from; future work may yet provide a means of subdividing them. Some neurones in all the groups were assumed to get monosynaptic excitation from the lateral geniculate and other thalamic nuclei. However, the input to deep layers is less rich than to layers 4 and 3 (Freund, Martin & Whitteridge, 1985*b*; Humphrey, Sur, Uhlrich & Sherman, 1985).

The different temporal form of the response to electrical stimulation depends on the poise of recurrent excitation *versus* inhibition. The differences in the response of the superficial and deep spiny populations could be best achieved by making the $GABA_A$ conductances a factor of 2 greater for the deep layer pyramids than for the superficial layer pyramids. This assumption has some support from the experiments reported below where the $GABA_A$ receptors were blocked. Alternative attempts to model the laminar differences by manipulating the strengths of the excitatory rather than the inhibitory inputs were less successful. In the following figures the simulations show the average response for all the neurones in each group. It is clear that the pattern of response of the two pyramidal neurone groups show strong generic similarities to the actual recordings shown in Fig. 2.

The functional weightings of the optimal microcircuit were as follows: pyramidal cells in layers 2+3 received half of their intracortical excitatory conductance from members of their own population, and the remainder from pyramidal cells in layers 5+6. A similar arrangement applied to pyramids in layers 5+6. The geniculocortical afferents supplied 10–20% of the total excitatory conductance to pyramids in layers 2+3 (P2+3), and 1–10% to pyramids in layers 5+6 (P5+6). The population of smooth neurones received half of its intracortical excitatory input from each of the two spiny populations. As for pyramids in layers 2+3, geniculocortical afferents supplied 10–20% of the total excitatory conductance to the smooth population. Typical values for the conductances are given in the Appendix. These were chosen so that the final behaviour of the microcircuit conformed to the range of values seen experimentally. Thus the modelled voltages and changes in input resistance are in good agreement with the experimental observations (e.g. Fig. 6).

Influence of parameters in the performance of the model

The microcircuit was sensitive to the relative activation times and the relative strengths of the excitatory and inhibitory populations (e.g. Fig. 11, below). If inhibition lagged or was too weak, then the intracortical excitation grew rapidly.

The intracortical excitatory connections within each group of pyramidal neurones were essential to the operation of the microcircuit. It is they that provided the means of amplifying an initially weak excitation of the superficial or deep groups of pyramidal neurones. The excitatory connections between the superficial and deep layer pyramids were functionally less critical for forming the pulse response modelled here (see below).

The fast $GABA_A$ component of inhibition was most effective in restricting the evolution of intracortical excitation. The early phase of the pulse response was sensitive to the poise of this $GABA_A$ component, and it was responsible for the differences in the temporal form of the response between superficial and deep layer pyramidal neurones (e.g. Fig. 6*E–F*).

The inhibitory feedback mediated by the $GABA_A$ component to the pool of

inhibitory neurones was not a critical parameter. (The $GABA_B$ component may turn out to be more significant because its longer time course could restrict the response of the inhibitory neurones to repetitive or rapidly changing input signals. These effects were not examined here.)

The performance of the microcircuit depended on the existence of a common pool of inhibitory neurones that were excited by thalamic afferents, and by superficial and deep layer pyramidal neurones. The existence of a common inhibitory pool had important consequences, for example, in addition to feedback inhibition, the deep layer pyramids received two stages of feedforward inhibition: one due to thalamic excitation of the inhibitory pool, the other due to the short-lived cycle of intracortical re-excitation of the superficial layer pyramidal neurones. In comparison, the contribution of the deep layer pyramids to the excitation of the inhibitory neurones was insignificant.

Action of GABA agonists and antagonists

A convenient way of testing the microcircuit was to block or activate components of the GABA receptors in actual cortical neurones and see whether the microcircuit would simulate the same behaviour. In all, 285 tests were performed during GABA ionophoresis, ninety-one with *n-m*-bicuculline, and twenty-seven with baclofen. In the first set of experiments we recorded the change in the intracellular response of eighteen neurones to electrical stimulation while the $GABA_A$ receptor antagonist, *n-m*-bicuculline, was applied ionophoretically onto the neurone. The results are shown in Fig. 6 for four neurones. The top trace in each case shows the control response, the middle trace the developing response, and the bottom trace the full-blown response.

The full-blown response to *n-m*-bicuculline took 5–10 min to evolve and took even longer to subside to control levels. In many cases we halted the ionophoresis after several minutes because the recovery from *n-m*-bicuculline application was so long and under the conditions of intracellular recording we hoped to obtain several trials for a single neurone. In some cases the intracellular recording was lost before the response returned to control levels. In all cases a similar pattern evolved during the *n-m*-bicuculline application, and reversed during recovery. Initially the size of the EPSP grew, and in some cases produced an action potential where none was before. With time, the size of the depolarization grew, giving rise to multiple action potentials, and in some cases became extremely broad (100 ms, see Fig. 6*A*). A late hyperpolarizing IPSP then terminated the *n-m*-bicuculline-enhanced depolarization.

Thus, the *n-m*-bicuculline appeared to eliminate the early part of the IPSP, allowing more excitation to predominate. The late part of the IPSP was insensitive to the bicuculline even with prolonged application. These data suggest the presence of two separate GABA receptors. The fast onset and short duration component of the IPSP is probably due to the bicuculline-sensitive $GABA_A$ receptors, while the slower onset, longer-lasting component is probably due to the bicuculline-insensitive $GABA_B$ receptors. With respect to our assumption that the $GABA_A$ conductance was two-fold greater in the deep layer pyramids, the pattern of response could be changed to a 'superficial' pattern through the moderate application of *n-m*-bicuculline. This is seen in Fig. 6*A* where the control response (top trace) has the pattern of a deep layer pyramid, with little initial EPSP and a rapidly developing IPSP. After moderate *n-m*-bicuculline application the EPSP became more pronounced and the

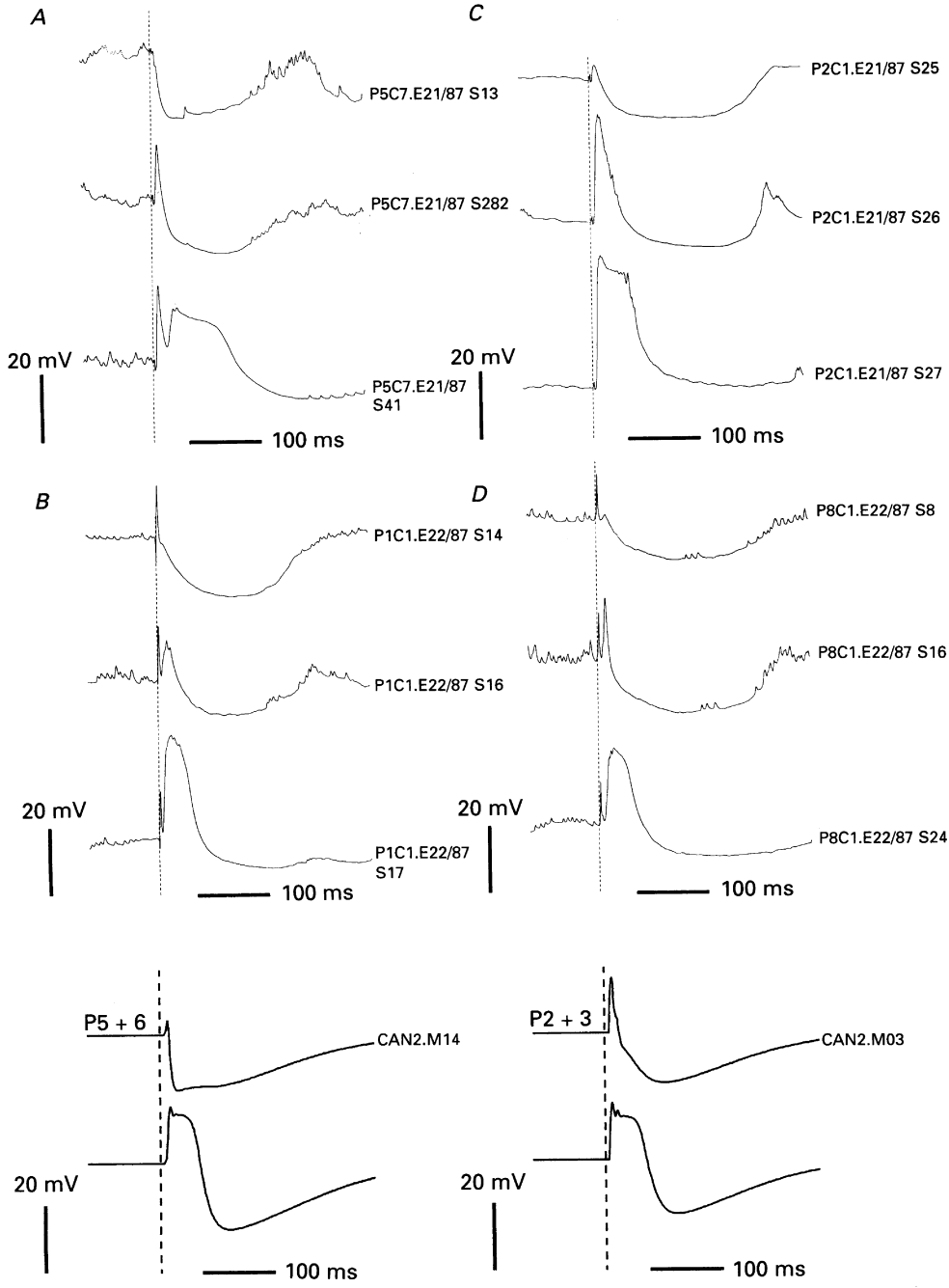

Fig. 6. Evolution of response to electrical stimulation during *n-m*-bicuculline application. One deep layer neurone (*A*) and three examples of superficial neurones (*B–D*) are illustrated. In all neurones the major change induced by $GABA_A$ receptors is an increase in the amplitude and duration of the EPSP. The late portion of the IPSP remained *n-m*-bicuculline insensitive, despite lengthy ionophoretic application in some cases. *E* and *F*, responses of model neurones to simulated application of *n-m*-bicuculline. As in the actual neurones, both superficial (P2+3) and deep pyramidal neurones (P5+6) show marked changes in the amplitude and duration of EPSPs compared to controls.

IPSP evolved more slowly to the maximum hyperpolarization, as in superficial layer pyramids.

The effect of *n*-*m*-bicuculline is thought to be reasonably local, affecting a small group of cells, at least with short periods of ionophoresis. In our experiments, for

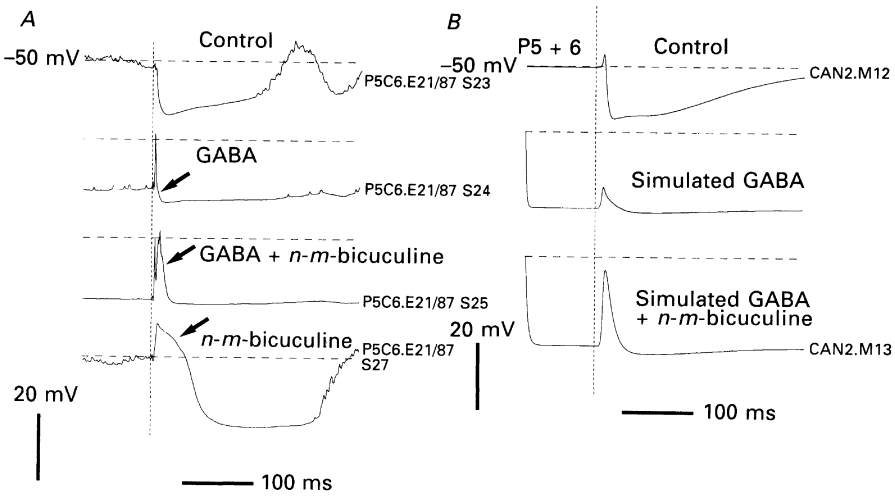

Fig. 7. *A*, response of deep layer neurone to application of GABA and bicuculline. Top trace shows control response. Second trace shows response during application of GABA. Third trace shows response after GABA plus *n*-*m*-bicuculline. Late EPSP revealed by bicuculline (arrowed). Bottom trace shows response with *n*-*m*-bicuculline only. Dashed lines show −50 mV control potential. *B*, response of model neurone from deep layer population to simulated application of GABA and *n*-*m*-bicuculline. Top trace shows control. Second trace shows response during simulated GABA application. Bottom trace shows response during simulation of GABA plus *n*-*m*-bicuculline application.

instance, the tip of the ionophoresing pipette was only 20–30 μm from the recording tip. This localized effect of ionophoresis of *n*-*m*-bicuculline was stimulated in the model by modifying the synaptic conductances in a subset of pyramidal and smooth cells in the appropriate layers. In this subset the effect of bicuculline was simulated by reducing the $GABA_A$ component of the inhibitory conductance to 20% of its original value. The simulations for examples of the superficial and deep layer pyramids are shown in Fig. 6*E* and *F*. They reflect quite accurately the response obtained in the actual neurones.

A second test of the model was to ionophoretically apply GABA ($n = 40$ neurones), or GABA in combination with *n*-*m*-bicuculline ($n = 14$), onto the neurone. The recovery to control levels after application of GABA was extremely rapid, occurring virtually as the ionophoretic current was being turned off. Figure 7*A* shows an example of a combined GABA and *n*-*m*-bicuculline experiment. The control (top trace) shows the response pattern of a deep layer pyramidal neurone. When GABA is applied the membrane hyperpolarizes from −50 to −66 mV (second trace). The early EPSP became more prominent, but the absolute amplitude of the IPSP

decreased, presumably because even the unstimulated membrane was now close to the GABA reversal potential. *n-m*-Bicuculline was then applied in addition to the GABA. The neurone hyperpolarized still further, but, in addition to the early EPSP, a later EPSP was also revealed (third trace, arrowed). When the GABA application

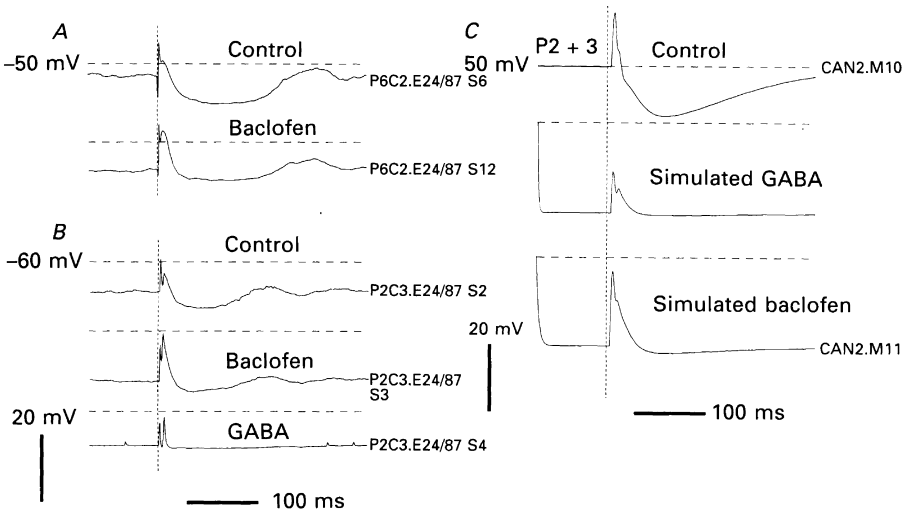

Fig. 8. *A* and *B*, response of superficial layer neurones to application of baclofen or GABA. Dashed line indicates −50 mV potential for the neurone in *A*, or −60 mV for neurone in *B*. *C*, response of model neurone from superficial population to simulated application of GABA or baclofen. Top trace shows control response. Second trace shows response during simulated GABA application. Lower trace shows model response during simulated baclofen application.

was stopped, the membrane depolarized to its control level and a full-blown *n-m*-bicuculline response was revealed (bottom trace). Thus, antagonism of the $GABA_A$ receptors during the GABA ionophoresis permitted additional excitation to reach the neurone during the period immediately following the stimulus. The additional hyperpolarization that occurred when the *n-m*-bicuculline was applied together with the GABA is presumably because blocking the chloride-mediated $GABA_A$ receptors allows the membrane to move towards the more negative $GABA_B$ (potassium-mediated) reversal potential. Note too in this example that the control trace is characteristic of a deep layer pyramidal neurone, whereas the *n-m*-bicuculline-only trace resembles more a superficial neurone, as was observed in Fig. 6*A*.

The response of a deep layer neurone to GABA and *n-m*-bicuculline was then simulated using the model. To simulate the GABA response, 50% of the $GABA_A$ and $GABA_B$ conductances were activated in the test neurones. The *n-m*-bicuculline effect was modelled as described for Fig. 6 above. The results of the simulations are shown in Fig. 7*B*. The top trace shows the control response. With the simulated application of GABA the model neurone hyperpolarizes and the size of the EPSP increases slightly. When the application of *n-m*-bicuculline plus GABA is simulated, the model

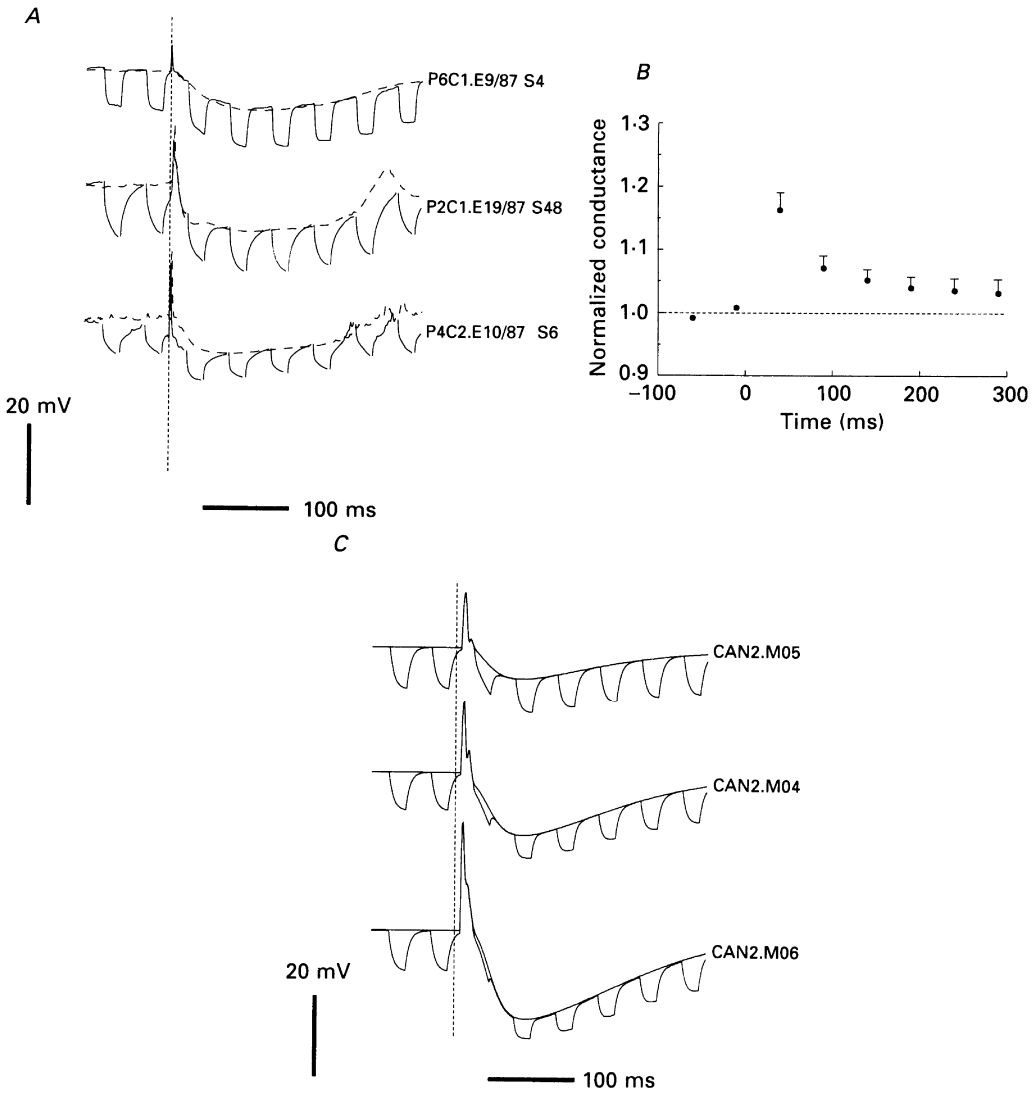

Fig. 9. *A*, measurement of changes in input resistance of three neurones during the averaged response to electrical stimulation. Note that amplitude of voltage deflections produced by constant-current pulses (−0·1 nA) does not vary substantially between control and response. *B*, changes in input conductance for all the neurones measured ($n = 32$). The maximum increase in conductance (equivalent to a decrease in input resistance) occurs immediately following the afferent stimulation ($t = 0$). Ordinate, time (ms); abscissa, conductance normalized to mean of the two current pulse responses in the control period. *C*, measurements of input resistance by simulating current-pulse injections in a model neurone of the superficial layers during the simulated pulse response. The traces show the response to increasing 'afferent' stimulus strengths (top to bottom; not tested *in vivo*). The simulated injected pulse is a constant current for all traces. As in the actual neurones, the maximum change occurs during the initial phase of the response.

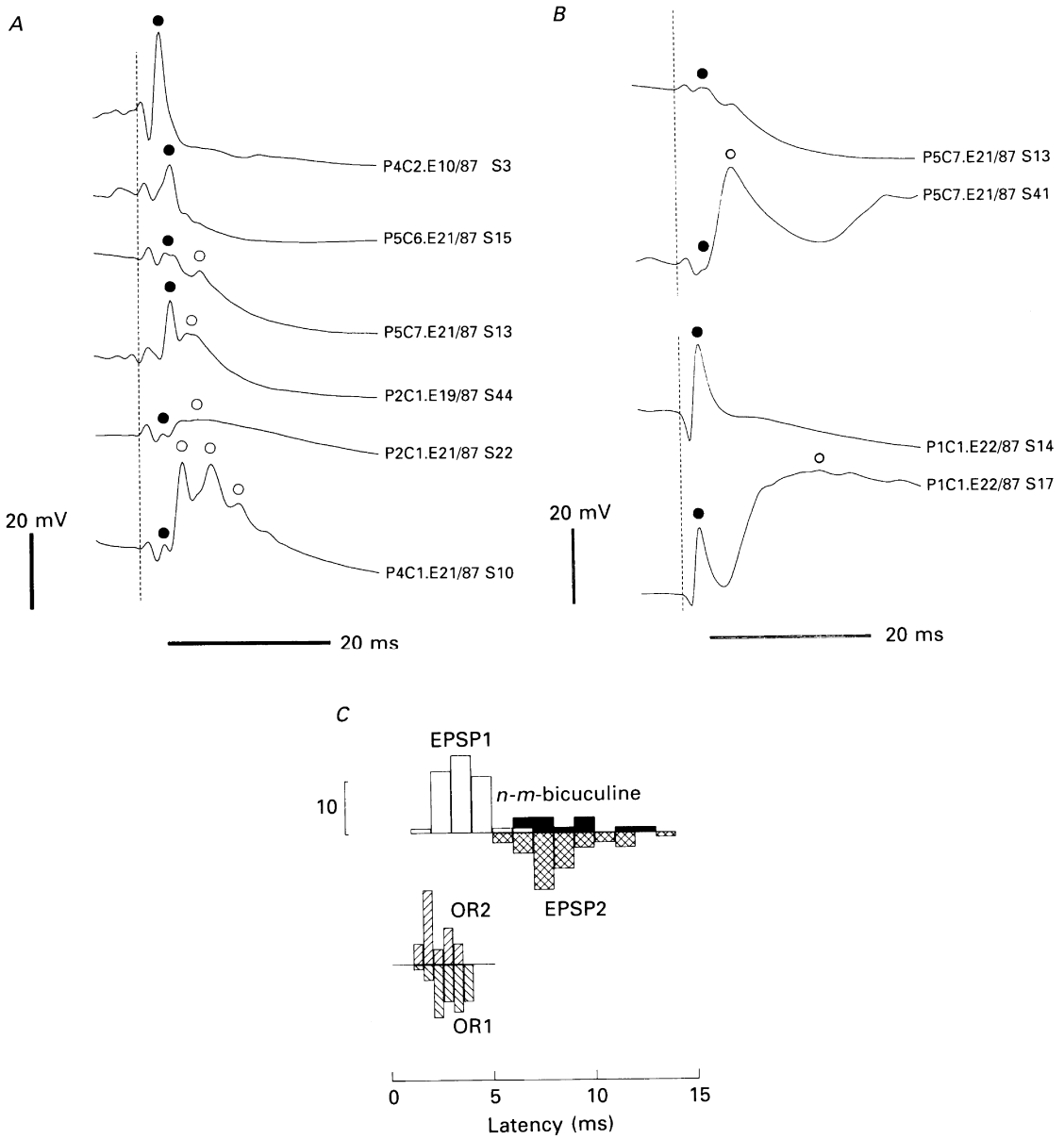

Fig. 10. *A*, expanded time views of the early portion of the evoked response for six different neurones. These traces were digitally filtered (see Methods). In most cases there are at least two separable peaks of depolarization. The latency to the peaks (●, thalamic excitation; ○, polysynaptic excitation) were measured for the histogram shown in *C*. *B*, changes in evoked responses during application of *n*-*m*-bicuculline, shown for two neurones. Uppermost trace for each pair is the control, lower trace obtained during *n*-*m*-bicuculline application. Note that the amplitude of the early depolarization (●) does not increase during application, but the late component increases greatly (○). *C*, upper histograms show latency to peak of EPSPs evoked by OR1 or OR2 stimulation. Open

neurone hyperpolarizes further and the size of the EPSP increases. These features agree well with the changes seen for the actual neurone illustrated in Fig. 7*A*.

A final test for the model was the action of the $GABA_B$ agonist, baclofen. Seven neurones were examined, with similar results obtained for all. The recovery time from baclofen was intermediate between that of GABA and *n-m*-bicuculline. Figure 8*A* and *B* illustrates, for two neurones with typical superficial layer pyramid patterns, the effect of ionophoresis of baclofen. In both cases the membrane hyperpolarizes, the EPSP becomes more prominent, and the late component of the IPSP flattens. The response of the neurone in Fig. 8*B* to GABA is also shown. The GABA response differs from the baclofen response in that the membrane does not hyperpolarize as much from the control value and the GABA is more effective in eliminating the IPSP fluctuations.

The baclofen effect was simulated by activating 50% of the $GABA_B$ conductances in the test neurones of the model. The results are shown for a superficial layer pyramid in Fig. 8*C*. The baclofen response (bottom trace) shows that the membrane hyperpolarizes in response to the $GABA_B$ receptor activation, so revealing more of the EPSP and flattening the IPSP. For comparison, the middle trace shows the simulated effect of applying GABA to the model neurone, where the additional activation of the $GABA_A$ component reduces the amplitude of the early EPSP. The baclofen simulation differs from the actual neurone shown in Fig. 8*A* only in that the activation of the $GABA_B$ receptors appears to be more effective in the simulation. In other respects the action of the baclofen agrees well with the simulated response.

Changes in input resistance

A further aspect of the model that could be investigated and compared with the performance of actual cortical neurones was the change in input resistance of the model neurone during the response to the input pulse. The change in input resistance is shown for a sample of three cortical neurones (Fig. 9*A*). The change in amplitude of the voltage deflections from the control to the response is not marked. The mean change in the input conductance for all thirty-two neurones tested is shown in Fig. 9*B*. The maximum change occurs early in the IPSP (earliest measure taken at 50 ms) and then declines monotonically. The maximum mean change in input conductance was an increase of about 16%. For the model, we found a similar pattern; the maximum change in the input resistance occurred early in the response. However, the size of the change was related to the magnitude of the input pulse (Fig. 9*C*). As the stimulus strength increased, the input resistance during the early phase of the simulated IPSP decreased, as has been observed *in vivo* (Dreifuss *et al.* 1969). The circuit compensates for increases in excitation by increasing the strength of the inhibition, which cuts off the EPSP. It should be noted that the increase in conductance in the simulations is mainly due to an increase in the excitatory conductance, not the inhibitory conductance. In real neurones most of the excitation arrives on the heads of spines and so part of the excitatory conductance would be masked from the dendritic trunk.

bars, earliest or first EPSP; cross-hatched bars, later or second EPSP; filled bars *n-m*-bicuculline-enhanced EPSP, which overlaps with EPSP2. Lower histograms show latency to base of earliest occurring action potential recorded extracellularly, evoked by OR1 or OR2 stimulation. Scale bar is 10 observations.

Inhibitory control of the intracortical excitation

The excitatory response to electrical stimulation revealed a number of depolarizing components (Fig. 10*A*). We examined these in the twenty-eight HRP-labelled neurones shown in Fig. 2. In the simplest analysis, we could dissect out two distinct

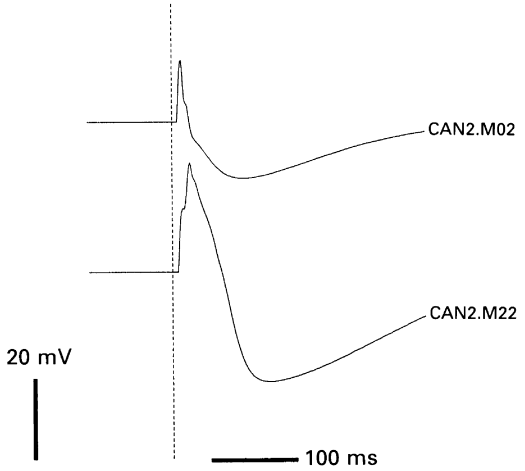

Fig. 11. Simulated effect of removing thalamic input to smooth (inhibitory) cell population. Top trace, control model response. Bottom trace, model response in which there is no direct thalamic input to smooth population, so preventing feedforward inhibition: only the feedback inhibition from the intracortical pathways acts to stop the excitatory response.

EPSPs, one with a peak at 3·4 ms ($n = 24$), the other with a peak at 8·6 ms ($n = 14$). The later peak was characteristic of superficial layer neurones (10/12), but occurred infrequently in deep layer neurones (4/15). We assumed that the first peak reflected the lateral geniculate afferent excitation, because it corresponded to the latencies of the earliest occurring action potentials measured extracellularly (Fig. 10*C*). The second peak would then reflect the intracortical excitation. We were concerned to see whether blocking the $GABA_A$ receptors would have a differential effect on these two components. Figure 10*B* shows the result when *n*-*m*-bicuculline was applied ionophoretically onto the neurone. The top trace shows the control, where both components are small. Ionophoresis of *n*-*m*-bicuculline (second trace) produces a marked increase in the size of the second component. The second neurone shows a similar effect. Before application of *n*-*m*-bicuculline the first EPSP is large, and the second shows only as a small inflexion. During *n*-*m*-bicuculline application the size of the first EPSP decreased, if anything, while the second EPSP grew enormously. *n*-*m*-Bicuculline elicited a large second EPSP even in those neurones in which none was obvious before. The coincidence in the latency to peak of the *n*-*m*-bicuculline-enhanced EPSP and the latency to peak of the second EPSP is shown in Fig. 10*C*. All of the *n*-*m*-bicuculline-enhanced EPSP latencies occurred after the peaks of the first EPSP. The latency to the inflexion point of the first action potential, stimulated from OR1 or OR2, is shown in the lower histogram. This indicates that the earliest

action potential occurs well before the second EPSP, and the *n-m*-bicuculline-enhanced EPSP, and supports our assumption that the second EPSP is cortical in origin.

We found that the first EPSP was largely unaffected by application of *n-m*-bicuculline. These data also suggest that the cortex is not subject to a significant amount of tonic inhibition. If cortical cells were, then $GABA_A$ blockade ought to change the amplitude of the first (presumed geniculate afferents) and the second EPSP (presumed intracortical). On the other hand, if inhibition is not tonic, but is also evoked by the lateral geniculate afferent excitation, then the first EPSP will be unaffected by $GABA_A$ blockade because the cortical cells are not subject to inhibition at the time of arrival of that input. The second EPSP will be affected, since it is the $GABA_A$ inhibition that restricts the degree of cortical re-excitation.

If cortical excitation is controlled by transient rather than tonic inhibition, then the relative timing of activation by thalamocortical afferents of spiny and smooth populations is likely to be critical. There was no experimental manoeuvre *in vivo* by which we could alter the phase relationship between the activation of the spiny and smooth populations. However, it was possible to simulate this experiment using the model. If there is no direct thalamocortical input to the smooth cells, and they depend on the excitation of intracortical connections, then cortical re-excitation cannot be adequately controlled (Fig. 11). The late excitation component becomes prominent, similar to the case in which $GABA_A$ inhibition is blocked by *n-m*-bicuculline (Fig. 10). It is essential that the thalamocortical afferents activate the smooth cells synchronously with, or slightly earlier than, the spiny cells if cortical re-excitation is to be restricted.

DISCUSSION

Our previous papers in this series (Berman *et al.* 1991; Dehay *et al.* 1991; Douglas *et al.* 1991) have shown that intracortical inhibition in the presence of visual stimulation is much less in evidence than was hitherto supposed from extracellular recordings. In contrast, using electrical stimulation of the thalamic afferents we found that robust IPSPs of long duration could be elicited in every neurone we studied. Thus, even though the machinery for substantial inhibition is available to each neurone, it appears that during visual stimulation only a fraction of the inhibitory capacity is used at any one time.

Characteristics of the IPSP

The cortical IPSPs are mediated by GABA (Kelly & Krnjević, 1969). In the present study we found two components to the IPSP, which correspond to the known characteristics of the $GABA_A$ and the $GABA_B$ receptors. The $GABA_A$ component could be blocked using the specific antagonist *n-m*-bicuculline, which is known to disrupt the responses to visual stimuli (Sillito, 1975, 1979; Tsumoto, Eckart & Creutzfeldt, 1979). The $GABA_B$ receptors were activated by baclofen. Using the drugs in combination we showed that the $GABA_A$ component was dominant early in the IPSP, but that the $GABA_B$ component was dominant later. The early phases of the IPSP were associated with a higher conductance change than the late phase, as

has been observed previously *in vivo* by Dreifuss *et al.* (1969) and *in vitro* by many workers including Berman, Douglas & Martin (1989).

At the membrane potentials recorded here (40–60 mV), both components of the GABA response were hyperpolarizing. However, the reversal potentials of the two receptors were clearly different. If the $GABA_A$ receptors were blocked during application of GABA, the membrane hyperpolarized, indicating that the $GABA_B$ component was more hyperpolarizing than the $GABA_A$ component. This was expected on the basis of the ion species that are thought to mediate the two responses. $GABA_A$ is probably mediated by chloride ions, with a reversal potential of about −70 mV, whereas the $GABA_B$ response is probably mediated by potassium ions, which have a reversal potential of about −85 mV (Eccles, 1964; Newberry & Nicoll, 1985).

Structure of the cortical microcircuit

The characteristics of the IPSP were incorporated in the functional microcircuit, which simulated the experimental results with remarkably high fidelity, given the simplifying assumptions that were made. The microcircuit has a strong resemblance to previous suggestions of cortical connections based on Golgi-stained neurones (e.g. Lund, Henry, MacQueen & Harvey, 1979) or HRP-filled neurones (Gilbert & Wiesel, 1979). However, there are several obvious points of difference. One is that the geniculate input excites monosynaptically more neurones than previous circuits allowed. The reason is simply that the additional connections exist: anatomical and physiological studies (Bullier & Henry, 1979; Ferster & Lindström, 1983; Martin & Whitteridge, 1984; Freund *et al.* 1985*b*; Freund, Martin, Somogyi & Whitteridge, 1985*a*) show that neurones in layers 3–6 can be activated monosynaptically by the X- and Y-type afferents. The W-afferents terminate in layers 1, 3 and 5 (Leventhal, 1979) and thus may contribute a further monosynaptic thalamic input to neurones in all layers.

The result is that the vast majority of neurones in all layers have a portion of their dendritic tree located in a zone of geniculate afferent termination. Thus virtually every neurone could receive a monosynaptic input from thalamic afferents, although the degree of innervation might vary between neuronal types (see White, 1989 for further discussion). In this context it should be noted (Fig. 4*C*) that some neurones in the microcircuit do not receive a monosynaptic input. Moreover, in the simulations we report the average properties of the group, not the properties of isolated individual members of the group.

A second point of difference from previous designs is that we have integrated the smooth neurones into the circuit. The problem was to decide how this could be done, because about seven different types of smooth neurones can be differentiated on the basis of their axonal arborizations (Lund *et al.* 1979; Peters & Regidor, 1981; Somogyi & Martin, 1985; Somogyi & Soltész, 1986; Somogyi, 1989). The main site of termination of the smooth neurone synapses is on the axon initial segment, the soma and the proximal dendrites and spines. The functions of these different types has been a fertile source of speculation (see Martin, 1984, 1988; Somogyi & Martin, 1985; Somogyi, 1989), but experimentally we know only that they have normal receptive field properties (Gilbert & Wiesel, 1979; Martin *et al.* 1983; Kisvárday, Martin, Whitteridge & Somogyi, 1985; Kisvárday *et al.* 1987) and in contrast to

pyramidal neurones, do not show strong adaptation to sustained excitatory input (McCormick, Connors, Lighthall & Prince, 1985). A theoretical study of chandelier and basket cells (Douglas & Martin, 1990) did not reveal qualitative differences between axo-axonic *vs.* somatic-proximal dendritic inhibition. At present we have no functional basis for differentiating between the smooth neuronal types and thus for the purposes of the simulation we have included them all in a single group.

Variations in the intrinsic membrane properties have not been modelled here (Connors, Gutnick & Prince, 1982; McCormick *et al.* 1985; Schwindt, Spain, Foehring, Stafstrom, Chubb & Crill, 1988*a*, *b*). It is likely that they do contribute to some extent, but the differences between the superficial and deep layer pyramidal cells that we observed for the pulse responses are unlikely to be strongly influenced by these intrinsic properties. For example, the early excitation seen in the superficial layer pyramidal neurones must be synaptic. It cannot be explained by membrane conductances that produce a burst discharge, because the intrinsically bursting neurones are found predominantly in layers 4 and 5 (Connors *et al.* 1982; McCormick *et al.* 1985). Many deep layer pyramids do not have an early excitatory discharge, so the protracted hyperpolarization that we observed in these neurones following pulse stimulation must be synaptically induced. Our ability to manipulate the hyperpolarizing phase using GABA receptor agonists and antagonists also suggests that extrinsic (synaptic) rather than intrinsic mechanisms are responsible for the dominant responses we observed.

The interaction of excitation and inhibition

Inhibition and excitation are inseparable in the cortical circuits. We found that stimulation of the thalamic afferents leads to the monosynaptic activation of both excitatory and inhibitory neurones, as predicted from structural studies (Freund *et al.* 1985*a*). In the present study, the experimental results showed that the spiny neurones could be differentiated into two physiological groups that were strongly correlated with laminar location. The excitatory depolarization of pyramidal cells in the deep cortical layers (5+6) was usually limited to the first 6 ms following stimulation. In contrast, the superficial layer (2+3) neurones usually had a long-lasting depolarization (often some 30 ms in duration), suggesting either a strong polysynaptic excitatory input or less early inhibition. This observation was unexpected because extracellular recording had shown that layer 5 contained neurones that responded to electrical stimulation with the longest latencies of any cells in the striate cortex (Bullier & Henry, 1979; Martin & Whitteridge, 1984). However, Martin & Whitteridge (1984) recorded extracellularly from many neurones in layer 5 that were difficult to excite using electrical stimulation, which suggests that strong inhibition might be present. However, it should be noted that layer 5 does contain monosynaptically activated neurones (Hoffman & Stone, 1971; Bullier & Henry, 1979; Ferster & Lindström, 1983; Martin & Whitteridge, 1984).

Evidence for strong inhibition in the deep layer neurones was found using intracellular recording. In superficial layer pyramidal neurones the hyperpolarizing IPSP took at least 100 ms to develop to its maximum depth of modulation. In deep layer pyramidal neurones the maximum was reached within 30 ms. This rapid hyperpolarization might have been due to a relative absence of afferent excitation to deep pyramids during the first 30 ms. However, we found that strong excitation was

available during this early phase (Fig. 6*A*). When the $GABA_A$ receptors were partially blocked in deep layer pyramids, their pattern of response came to resemble that of the superficial layer pyramids. These data suggested that the early inhibition of deep pyramids must be stronger than that of the superficial layer pyramids and this aspect was incorporated in the model. The physiological results also show that both the early and the late components of the IPSP are hyperpolarizing, even when the control membrane potentials are around −60 mV. Thus, the conditions required for 'silent' inhibition (Koch & Poggio, 1985*a*), where the membrane potential and the reversal potential of the ions mediating the inhibition are the same (see Dehay *et al.* 1991), do not occur in visual cortex.

The long duration of the IPSP offers an explanation for the 'trailing edge' phenomenon we noted using moving visual stimuli (Berman *et al.* 1991; Douglas *et al.* 1991). We found that hyperpolarizing inhibition would follow a strong response to the optimal stimulus, and that this inhibition was not contrast dependent; it occurred with both light and dark bars even in simple receptive fields. It may simply be a post-train hyperpolarization arising from intrinsic membrane currents (Schwindt *et al.* 1988*a*, *b*). Another explanation is that the visual stimulus excites both excitatory and inhibitory neurones, but because the time course of the excitatory potentials is much shorter than the $GABA_B$-mediated potentials, the inhibitory hyperpolarization outlasts the depolarization produced by the excitation. This phenomenon is seen in simulations using the microcircuit, where the conductances necessary to produce after-train hyperpolarizations were not included (see below).

Models of receptive fields have relied on the thalamic inputs to shape the form of the receptive field. The best example of this form is the Hubel & Wiesel (1962) model for orientation selectivity in simple cells, which has recently been the subject of a computer simulation (Ferster, 1988). In their model Hubel and Wiesel proposed that geniculate excitation alone is responsible for the orientation tuning of simple cells. Although the simulation showed that the model could replicate the orientation response under a restricted set of conditions (Ferster, 1988), more varied test conditions have shown that a purely excitatory model cannot explain the degree of orientation selectivity or the gain control seen in cat cortical neurones (Wehmeier, Dong, Koch & Van Essen, 1989).

Incorporating inhibition into the orientation circuitry provides a better match to the experimental data (see e.g. Wehmeier *et al.* 1989). The considerable experimental evidence for inhibition in orientation is reviewed by Martin (1988). Unfortunately, none of the models that do include inhibitory components can explain the present observations. They either postulate circuitry that does not seem to exist, or physiological processes that are not seen (see Martin, 1988; Berman *et al.* 1991; Douglas *et al.* 1991). The experiments and model presented here offer an alternative interpretation of the manner in which the selective responses of cortical neurones might be generated.

Thalamic excitation and intracortical amplification

A detailed view of the initial excitatory phase that followed thalamocortical stimulation revealed two separable components. The first was a short latency EPSP, often associated with an action potential, and probably due to monosynaptic

excitation by lateral geniculate afferents. In most of the superficial pyramids, but in only a few deep pyramids, the short latency EPSP was followed by more prominent depolarization, which lasted for some 30 ms before being cut off by the IPSP. The long latency, duration, and large amplitude of this late EPSP made it unlikely that it arose directly from the original afferent volley, and was probably due to polysynaptic activation from other cortical neurones. In the model the thalamic and cortical components of excitation could be unambiguously identified, and the longevity of the late EPSP in superficial layer neurones could be explained by the excitatory and inhibitory interactions within the cortical circuit.

In the hypothetical microcircuit, the connections from other cortical neurones provide most of the excitatory current arriving at the neurone. This is because a small thalamic input can be greatly amplified by the massive divergence in the intracortical connections of excitatory neurones (Gilbert & Wiesel, 1979; Martin & Whitteridge, 1984; Kisvárday *et al.* 1986; Gabbott *et al.* 1987). The simulations and the experimental results using the $GABA_A$ blocker, *n-m*-bicuculline, indicate that control of the intracortical re-excitation has to take place at the earliest stage of cortical processing to prevent over excitation. Inactivation of the $GABA_A$ receptors leads to a selective enhancement of the late (amplifiable) component of the excitatory response, but has little effect on the thalamic EPSP, because there is no tonic inhibition: cortical neurones are generally silent (Gilbert, 1977). Controlling intracortical amplification does not depend entirely on activation of the $GABA_A$ mechanism by the thalamocortical volley, however. The spiny neurones also provide synaptic input to the smooth cells (McGuire, Hornung, Gilbert & Wiesel, 1984; Kisvárday *et al.* 1986; Gabbott *et al.* 1987; Somogyi, 1989), and these pathways provide the means for feedback control of the amplification.

If the thalamic excitation is small, as we have assumed, the amount of inhibition needed to suppress it would also be small. The behaviour of the microcircuit shows that if the activation of smooth cells is synchronous with, or slightly earlier than, the spiny cells, then cortical re-excitation can be minimized. This may explain why the geniculocortical afferents tend to make contact directly with the somata of smooth cells, and why these afferents are myelinated almost up to the terminal boutons (Freund *et al.* 1985*a*), an observation that suggests the necessity to ensure secure and rapid activation of the GABAergic neurones.

The ability to restrict cortical re-excitation is very significant since it means that inhibition is not required to suppress full-blown excitation. Instead, the restriction reduces the excitatory load that inhibition must oppose. This accounts well for the difficulty in detecting significant inhibition with non-optimal stimuli (Ferster, 1987; Douglas *et al.* 1988, 1991; Berman *et al.* 1991). A simple analogy illustrates the principle: the thalamic excitation ignites the touch paper of intracortical excitation. If the lighted touch paper is not quenched by cortical inhibition, then the apparatus of cortical excitation can fire off. Controlling the *inhibitory* neurones is therefore one of the keys to controlling cortical excitation. Our knowledge of the connections and physiological interactions of the different types of GABA neurones is minimal. This will be an important area of future investigation.

Demonstration of functional competence of the microcircuit

To demonstrate the explanatory power of the microcircuit, we have taken the example of the direction-selective neurones that receive monosynaptic input from non-directional thalamic neurones. This we believe is the most difficult example to

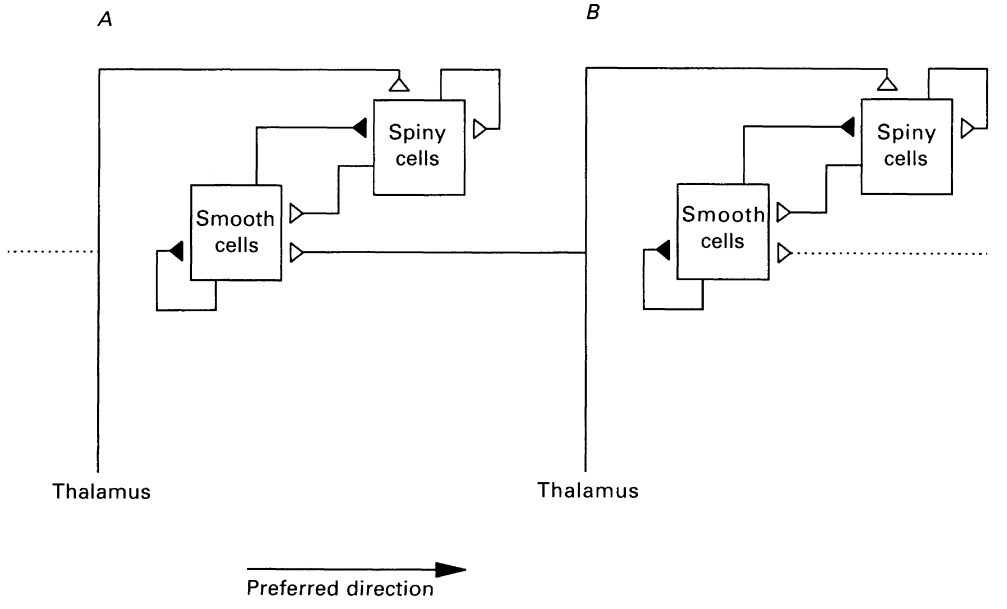

Fig. 12. Block diagram of circuit that models the intracellular recordings from cortical neurones during direction selective behaviour. Thalamic afferents stimulate two subcircuits (*A* and *B*) that are similar to the canonical model shown in Fig. 5. In each subcircuit two populations of neurones interact with one another: one population is inhibitory (smooth cells, filled synapses), and the other is excitatory (spiny cells, open synapses). The thalamic afferents excite the smooth cell populations of subcircuits to the left, and the spiny cell populations of subcircuits to the right. When activity in the thalamic afferent of *A* precedes that of *B* (preferred direction), the spiny population in *A* is activated and expresses its recurrent excitation. The maximum discharge of the spiny population is restricted by interaction with its smooth cell population. When activity in the thalamic afferent of *B* precedes that of *A* (non-preferred direction), the smooth population in *A* is activated and suppresses its spiny population during the arrival of thalamic excitation to the spiny population in *A*. In this model the major component of excitation that is observed in spiny cells during the preferred response is due to cortical re-excitation. The thalamic input provides a relatively small initial component that is easily controlled by inhibition in the non-preferred direction. Dotted lines indicate that the microcircuits may be repeated in a crystal-like structure.

account for in terms of conventional ideas of the generation of stimulus-selective receptive fields, since the thalamic excitation is identical for both directions of motion, only the timing of the inputs is different. In conventional explanations, direction selectivity is obtained by inhibiting the strong excitatory drive from the thalamus when the stimulus moves in the non-preferred direction. As we have discussed (Introduction; see also Koch *et al.* 1990) the problem is that the degree of

inhibition required in these conventional explanations is not seen using intracellular recordings. The microcircuit can explain this.

We have linked two modules, each containing the identical microcircuit, in the manner illustrated in Fig. 12. To simplify the computations we consider only neurones in layer 4, but the same principles apply for the whole circuit. The only manipulation required to generate direction selectivity is to activate the smooth cell groups with thalamocortical afferents whose receptive fields are slightly displaced from those of the thalamocortical afferents supplying the spiny cells in the same module. When the bar moves in the preferred direction the spiny neurones are excited slightly ahead in time of the smooth neurones they excite, while in the non-preferred direction the smooth neurones are excited slightly before the spiny neurones they inhibit. The slight advantage given to one of the two competing groups of neurones then determines the outcome. If the excitatory neurones are stimulated first by the thalamic afferents then they produce strong cortical re-excitation that cannot be inhibited by the smooth cells. If the inhibitory group is excited first then it will prevent the thalamic excitation from igniting the intracortical re-excitation, and the resultant response will be minimal.

The net synaptic currents that arrive at the soma–axon hillock and the normalized conductance changes associated with these currents are given in Fig. 13. In the preferred direction of motion (upper traces) the net synaptic current recorded in the neurone is initially inward and leads to a depolarization and action potential discharge. After the discharge the nett current is outward, leading to a post-discharge hyperpolarization similar to that seen in actual neurones, here due to the extended time course of the $GABA_B$ response relative to the excitatory currents. Similar patterns were seen in our *in vivo* recordings (Berman *et al.* 1991; Douglas *et al.* 1991). The high conductances associated with this response are mainly due to the excitatory currents, which are modelled as coming directly onto the dendritic shafts. In actual neurones much of this conductance change would occur on the spine head and would be masked by the spine neck resistance.

In the non-preferred direction of motion (lower traces), the inhibitory neurones are activated before the thalamic afferents excite the spiny cells. The thalamic excitation is inhibited and re-excitation cannot be initiated. The nett synaptic current recorded in the neurone is inward and depolarizes the neurone about 4 mV. The conductance change is largely due to the activity of the inhibitory synapses and is about 20% of control, which is about the lower limit of what we could measure experimentally.

Since it is the time difference in the activation of the clusters of inhibitory and excitatory cells that determines the nett result, altering this timing will affect direction selectivity. The prediction from the model is that the direction selectivity will increase with velocity to a maximum at the velocity that produces the strongest response. With further increase in velocity the directionality will then decrease. This is exactly what has been found experimentally (Orban, Kennedy & Maes, 1981).

If the excitation were being delivered solely by thalamic afferents, as suggested by many models (e.g. Hubel & Wiesel, 1962; Heggelund, 1981; Ferster, 1987, 1988) then we can calculate the size of the inhibitory conductances that would be required to suppress the thalamic excitation and give the result we have illustrated for the non-preferred direction of motion. For shunting synapses with a reversal potential of

−60 mV, the inhibitory conductance would have to be 10 times the input conductance of the neurone. For hyperpolarizing synapses with a reversal potential of −80 mV the inhibitory conductance would have to be 1·8 times the input conductance. Conductances of such magnitude do occupy the realms of theory (Koch

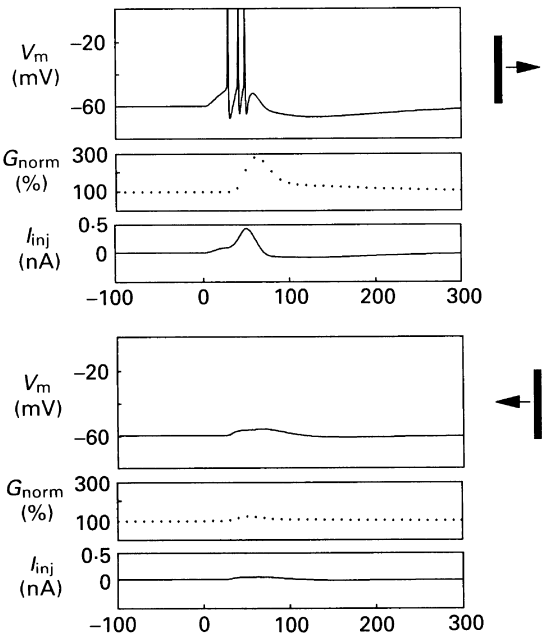

Fig. 13. Simulation of intracellular responses of a representative spiny neurone (in subcircuit *A*, Fig. 12) during preferred (upper traces) and non-preferred (lower traces) stimulation. During preferred stimulation the neurone generates action potentials in response to nett excitatory current (I_{inj}) that is largely a result of cortical re-excitation. In this model the excitatory synapses are applied directly to the dendritic trunk rather than to spines and so the increase input conductance (G_{norm}) is larger than would occur *in vivo*. During non-preferred stimulation there is only a 3·5 mV depolarization of the membrane potential, and the nett excitatory current is only a small fraction of that in the preferred direction. The increase in neuronal input conductance (G_{norm}) during non-preferred stimulation is small (21%), showing that large conductance changes are not necessary to achieve directional preference.

& Poggio, 1983), but have not even been hinted at in *in vivo* experiments (Ferster, 1986, 1987; Douglas *et al.* 1988; Berman *et al.* 1991).

It is important to note that in our realization of the cortical circuits that lie within a single module, the activity of the spiny and smooth cells operate in tandem, not opposition. From the design of the microcircuit it follows that strong re-excitation by the spiny cells will drive the smooth cells strongly. Weak re-excitation drives the smooth cells weakly. This means that the smooth cells, and the spiny cells they inhibit, can co-exist in the same cortical column and have similar selectivity. This is a crucial observation since every other inhibitory model of cortical selectivity makes the opposite prediction, i.e. a lack of response is taken as an indication of strong inhibition, while a strong response is taken to indicate that inhibition is absent (see

Martin, 1988). Our functional microcircuit also provides an explanation for the rich innervation by smooth neurones of their *own* cortical columns (Freund *et al.* 1983; Kisvárday *et al.* 1986, 1987; Martin, 1988; Martin, Friedlander & Alones, 1989). It also offers an explanation why the strongest inhibition in simple cells is evoked with optimal stimuli (see Figs 15 and 16 in Douglas *et al.* 1991).

Implications for future work

We have used a simple version of the microcircuit to explain our experimental observations in direction-selective neurones that receive a monosynaptic input from the non-directional thalamic afferents (Berman *et al.* 1991; Douglas *et al.* 1991). With little modification, and using the same principles of operation we can, in principle, account for other selectivities in cortical neurones, including orientation, end-inhibition and binocular disparity tuning. The core concept is that a small excitatory input (e.g. from thalamus, or claustrum, or from other cortical areas) to a cortical module is sufficient to set in motion a competitive interaction between highly interconnected groups of neurones within the column. The outcome of the competitive interaction is determined by the initial biases that are set up, as we have illustrated for the case of direction selectivity. The output of the module is determined by the collective action of localized groups of neurones, which evolve their solution over many milliseconds. In this view, analog processors (Mead, 1989) are more appropriate models for the action of the cortical circuits than the concepts of digital processing that have been dominant for the past two decades.

Many further elaborations are possible for the model. There are many cortical connections already mapped by us and others, whose influences we are beginning to explore, and which could eventually be incorporated in the microcircuit. The principles of operation of a cortical module elaborated here may be generalized to other cortical areas (Rockel, Hiorns & Powell, 1980) and could be tested using the methods we have employed for cat area 17. The microcircuit developed here is therefore a first step towards realizing a 'canonical' microcircuit for neocortex.

APPENDIX

Development and operation of a microcircuit for visual cortex

In order to make the problem computationally tractable and to achieve an abstraction from conventional functional models of visual circuits, we had to make several simplifications. We chose a pulse as the stimulus because it is independent of the specific attributes of visual stimuli. Pulse stimuli are widely used in the analysis of systems and have been used extensively in the analysis of neural circuitry. They have the additional advantage that they can be used to analyse circuitry in cortical areas whose natural stimulus requirements are not yet known. Here the electrical pulse stimulation was modelled by an α function (Jack *et al.* 1975).

Development of idealized, simplified model neurones

The second simplification we made was in the morphology of the neurones. The main components of the cortical circuits are the pyramidal neurones (approximately 70% of cortical neurones; Winfield, Gatter & Powell, 1980) and the smooth,

GABAergic neurones (approximately 20% of cortical neurones; Gabbott & Somogyi, 1986). The remaining neurones, which will not be considered here, consist of 'various' types, including the stellate cells and bipolar and fusiform neurones. The dendritic morphology of the smooth cells is so similar that the different types can

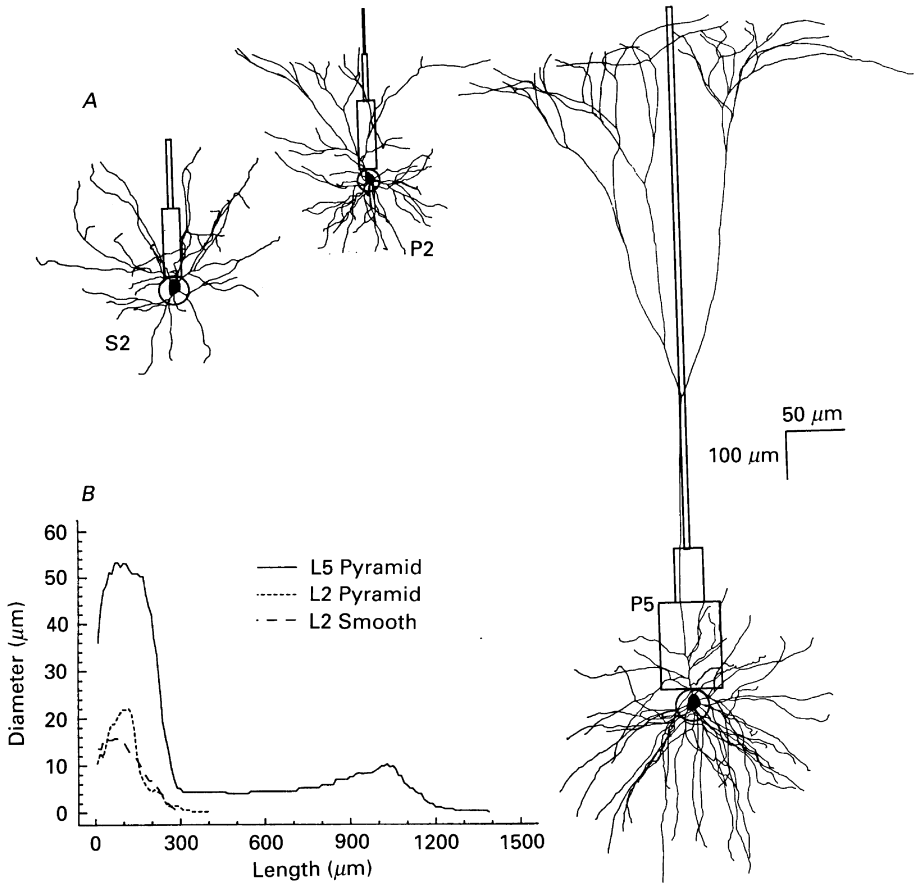

Fig. 14. *A*, montage of actual neurones used to develop idealized, simplified model neurones. Only dendrites are shown of layer 5 pyramid (P5), layer 2 pyramid (P2) and layer 2 smooth ('basket cell', S2) neurones. The compartmental model of each cell type used in the computer simulations is drawn over the original representative neurone. Each model cell consists of an ellipsoidal soma (shown here as spherical), and a number of cylinders that represent the dendritic tree. Dimensions of the ellipsoid and cylinders were obtained by three-dimensional reconstruction of the representative neurone. *B*, relative diameter *vs.* length for the actual neurones used to develop the idealized simplified model neurones. Note the overlap of the layer 2 spiny (pyramid) and smooth (basket) neurones.

only be discriminated on the basis of their axonal projections (Somogyi & Martin, 1985; Somogyi, 1989).

The pyramidal neurones have a very different morphology to the smooth neurones and vary considerably, particularly in the contribution of their apical dendrites (Ramón y Cajal, 1911; Gilbert & Wiesel, 1979; Martin & Whitteridge, 1984). In order

to make some accommodation for these anatomical differences without unduly complicating the computations, we simplified the morphologies of the various cell types represented in the model. We first reconstructed the three-dimensional structure of the soma and dendrites of three representative HRP-filled neurones; a layer 2+3 pyramidal cell, a layer 2+3 smooth (basket) cell, and a layer 5 pyramidal

TABLE 1. Comparison of input resistance in neurones using two different methods

		Cells		
Analysis	Morphology	L5+6 pyramid	L2+3 pyramid	L2 basket
Koch–Poggio	Detailed	21·4	96·3	102·2
	Simple	23·3	103·8	105·8
Compartmental	Simple	20·9	95·7	101·5

Comparison of input resistance (MΩ) in detailed and simplified morphology of cortical neurones, using the Koch–Poggio or compartmental methods. $R_m = 10$ kΩ cm²; $R_a = 0{\cdot}1$ kΩ cm.

cell (Fig. 14*A*). In theory (Rall & Rinzel, 1973; Rinzel & Rall, 1974) the dendritic tree can be collapsed into a simple equivalent dendritic cylinder provided that: (a) all terminal dendritic branches end at the same electrotonic length from the soma and (b) the 3/2 power branch relationship is upheld. We found that neither of these conditions held reliably for cortical cells, but that empirically a simplification was possible.

The cross-sectional area of all the dendrites were summed together at intervals of 10 μm displacement from the soma, and used to compute the diameter of an equivalent cylindrical dendrite (Fig. 14*B*). The equivalent diameter profiles were further simplified into two to three cylinders by averaging the diameters over selected serial regions of the profile. These cylinders, and the ellipsoidal somata, yielded the simplified representation of the cortical cell types used in the model (Fig. 14*A*).

The acceptability of this simplification was assessed by comparing the somatic input resistances of the neurones computed from their detailed morphology with that obtained from their simplified compartmental description. The input resistance of both descriptions was evaluated using the Koch–Poggio method (Koch & Poggio, 1985*b*). The simple description was also evaluated by the program CANON, using simulated current injection. The agreement was remarkably good (Table 1), particularly in view of the sweeping simplifications applied.

Simulation

Models of cortical circuits were investigated using a general neuronal network-simulating program, CANON (written by R.J.D.). This program permits the morphologies of neurones to be specified as sets of interconnected compartments. The passive, active, and ligand-gated conductances of each compartment can be specified, as well as the synaptic linkages and transmission delays between the output of a neurone and the compartments of its target neurones.

In this study we were concerned with the interactions between populations of neurones rather than between individual cells. Each population consists of a large

number of neurones whose morphological and functional properties are similar. It was impractical for us to simulate the detailed behaviour of all the neurones in such a population. Instead, the behaviour of each population was modelled by a single 'neurone' that represented the average of neurones belonging to that population.

All neurones were assumed to have both $GABA_A$ and $GABA_B$ receptors (Connors, Malenka & Silva, 1988; Douglas & Martin, 1990), indicated in Fig. 5 by filled triangle symbols, of the smooth neurone population. $GABA_A$ receptors were located on the soma and the proximal dendritic compartment, while $GABA_B$ receptors were located only on the latter. Excitatory interconnections are indicated by the open triangles. Here only a non-NMDA receptor was assumed. The excitatory synapses were located only on the dendritic compartment.

The synaptic conductances of cortical neurones and the time constants that govern their behaviour have yet to be determined experimentally. After examining the performance of the model over a range of parameters we chose a set of values that were consistent with those used in the literature (Jack *et al.* 1975; Getting, 1989), reflected the simplest assumptions, and optimized the performance of the model. Thus, the $GABA_A$ conductance of inhibitory synapses on pyramidal cells of layers 5+6 was made 2–4 times greater than that of superficial layer pyramids (P2+3) and smooth cells, so as to match the physiological performance. The $GABA_B$ conductance was the same in all populations. The performance of the model was relatively insensitive to recurrent inhibition of the smooth population. Typical absolute conductance values were as follows: total intracortical excitation in P2+3, 8 mS cm^{-2}; geniculocortical excitation to P2+3, 1 mS cm^{-2}; $GABA_A$ in P5+6, 1 mS cm^{-2}; $GABA_B$ in P5+6, 0·5 mS cm^{-2}. Reversal potential was −60 mV for $GABA_A$ and −80 mV for $GABA_B$. These are average membrane conductances. Since synapses do not cover the membrane surface uniformly, the conductance of the synaptic membrane will be larger than the values quoted here.

The morphology of the representative neurones was obtained by three-dimensional reconstruction (TRAKA, CelTek) of the soma and dendrites of suitable cortical neurones that had been labelled intracellularly with HRP. The detailed structures of the soma and dendrites were transformed into a simple equivalent neurone that consisted of an ellipsoidal somatic compartment, and three to four cylindrical compartments that represented the dendritic arbor (see Results). The small signal impedance properties of the detailed and simple representation were compared using the algorithm of Koch & Poggio (1985*b*; Koch *et al.* 1990).

The surfaces of the compartments represented the neuronal membrane and were assigned capacitance and conductances of various kinds known to be present in cortical cells. All compartments were assigned a passive leak conductance. The soma and proximal dendritic compartments also contained conductances that mediated the effect of excitatory and inhibitory inputs.

Since the neuronal populations were represented by their average neurone, action potential discharge was treated as a rate-encoded output rather than discrete spike events, and so the conductances associated with action potential generation and adaptation were not included in the model.

The following equations were used to model the behaviour of the neurones. The membrane potential of each compartment was defined as

$$C_m \, dV_m(t)/dt = -I_{comp} - I_m,$$

where V_m is the membrane potential (mV), C_m is the membrane capacitance (μF cm^{-2}), I_{comp} is the axial current contributed by adjacent compartments and I_m is the membrane current contributed by current compartment.

The axial currents depended on the voltage gradient between adjacent compartments, and the axial resistance of the cytoplasm. Terminal cylindrical compartments were assumed to have sealed ends (Rall, 1977). The membrane current was

$$I_m = I_{syn}(V_m t) + I_{leak}(V_m) + I_{inj}(t),$$

where I_{syn} is the synaptic current (nA), I_{leak} is the leak current (nA) and I_{inj} is the current injected via the electrode (nA).

These currents were defined as follows:

$$I_{leak} = g_{leak}(V_m - E_{leak}),$$

where g_{leak} is the leak conductance (μS cm^{-2}) and E_{leak} is the reversal potential of the leak conductance, and

$$I_{syn} = g_{max} s(t)(V_m - E_{syn}),$$

where g_{max} is the maximum conductance generated by a particular synaptic input (μS cm^{-2}), $s(t)$ is the normalized time course of a particular synaptic conductance, E_{syn} is the synaptic reversal potential. The time course $s(t)$ depended on the ratio of the actual presynaptic discharge rate to the maximum rate, and response time constants. For most synaptic inputs

$$ds/dt = f(t)/(f_{max}\tau_m) - s(t)/\tau_h,$$

where $f(t)$ is the presynaptic action potential discharge rate (spikes s^{-1}), f_{max} is the maximum presynaptic discharge rate (spikes s^{-1}), τ_m is the onset time constant (ms) and τ_h is the decay time constant (ms). However, the $GABA_B$ conductance change is thought to be mediated by an intermediate mechanism, possibly the cyclic GMP concentration, and so these inputs were modelled as

$$ds/dt = (x(t) - s(t)/\tau_s,$$

where

$$dx/dt = f(t)/(f_{max}\tau_m) - x(t)/\tau_h,$$

and τ_s is a slow time constant. The effect of electrical pulse stimulation of the geniculocortical afferents was modelled by an α function (Jack *et al.* 1975),

$$s(t) = (t/\tau_{peak}) \exp(-(t/\tau_{peak})),$$

where τ_{peak} is the time to peak of the conductance transient. The discharge rate was defined as

$$f(t) = f_{max}(1 - \exp(-(V_m - D_{thres})/D_{shape})),$$

where D_{thres} is the voltage threshold (mV above V_r, the resting membrane potential) and D_{shape} is the shape parameter.

The program CANON (CelTek) was executed on a 25 MHz 80386/80387 RM Nimbus VX (Research Machines), and simulated the 400 ms response to pulse stimulation and electrode current injection illustrated in Fig. 9 in 9 min.

We thank John Anderson for technical assistance, Mr Neil Berman for his advice in some of these experiments and the E. P. Abrahams Trust for support. R.J.D. acknowledges the support of the Guarantors of Brain, the MRC (South Africa), and the University of Cape Town. K.A.C.M. is the Henry Head Research Fellow of the Royal Society.

REFERENCES

Beaulieu, C. & Somogyi, P. (1990). Targets and quantitative distribution of GABAergic synapses in the visual cortex of the cat. *European Journal of Neuroscience* **2**, 296–303.

Berman, N. J., Douglas, R. J. & Martin, K. A. C. (1989). The conductances associated with inhibitory postsynaptic potentials are larger in visual cortical neurones *in vitro* than in similar neurones in intact, anaesthetized rats. *Journal of Physiology* **418** 107*P*.

Berman, N. J., Douglas, R. J., Martin, K. A. C. & Whitteridge, D. (1991). Mechanisms of inhibition in cat visual cortex. *Journal of Physiology* **440**, 697–722.

Bishop, P. O., Coombs, J. S. & Henry, G. H. (1971). Responses to visual contours: spatio-temporal aspects of excitation in the receptive fields of simple striate neurones. *Journal of Physiology* **219**, 625–657.

Bishop, P. O., Kato, H. & Orban, G. A. (1980). Direction-selective cells in complex family in cat striate cortex. *Journal of Neurophysiology* **43**, 1266–1283.

Bullier, J. & Henry, G. H. (1979). Ordinal position of neurons in cat striate cortex. *Journal of Neurophysiology* **42**, 1251–1263.

Connors, B. W., Gutnick, M. J. & Prince, D. A. (1982). Electrophysiological properties of neocortical neurons *in vitro*. *Journal of Neurophysiology* **48**, 1302–1320.

Connors, B. W., Malenka, R. C. & Silva, L. R. (1988). Two inhibitory postsynaptic potentials, and $GABA_A$ and $GABA_B$ receptor-mediated responses in neocortex of rat and cat. *Journal of Physiology* **406**, 443–468.

Dehay, C., Douglas, R. J., Martin, K. A. C. & Nelson, C. (1991). Excitation by geniculocortical synapses is not 'vetoed' at the level of dendritic spines in cat visual cortex. *Journal of Physiology* **440**, 723–734.

Diamond, J., Gray, E. G. & Yasargil, G. M. (1970). The function of the dendritic spine: a hypothesis. In *Excitatory Synaptic Mechanisms*, ed. Anderson, P. & Jansen, J. K. S. pp. 213–222. Universitetsforlaget, Oslo.

Douglas, R. J. & Martin, K. A. C. (1990). Neocortex. In *Synaptic Organisation of the Brain*, ed. Shepherd, G., pp. 220–248. Oxford University Press, New York.

Douglas, R. J., Martin, K. A. C. & Whitteridge, D. (1988). Selective responses of visual cortical cells do not depend on shunting inhibition. *Nature* **332**, 642–644.

Douglas, R. J., Martin, K. A. C. & Whitteridge, D. (1989). A canonical microcircuit for neocortex. *Neural Computation* **1**, 480–488.

Douglas, R. J., Martin, K. A. C. & Whitteridge, D. (1991). An intracellular analysis of the visual responses of neurones in cat visual cortex. *Journal of Physiology* **440**, 659–696.

Dreifuss, J. J., Kelly, J. S. & Krnjević, K. (1969). Cortical inhibition and gamma-aminobutyric acid. *Experimental Brain Research* **9**, 137–154.

Eccles, J. C. (1964). *The Physiology of Synapses*. Springer Verlag, Berlin, Gottingen and Heidelberg.

Ferster, D. (1986). Orientation selectivity of synaptic potentials in neurons of cat primary visual cortex. *Journal of Neuroscience* **6**, 1284–1301.

Ferster, D. (1987). Origin of orientation-selective EPSPs in simple cells of cat visual cortex. *Journal of Neuroscience* **7**, 1780–1791.

Ferster, D. (1988). Spatially opponent excitation and inhibition in simple cells of the cat visual cortex. *Journal of Neuroscience* **8**, 1172–1180.

Ferster, D. & Lindström, S. (1983). An intracellular analysis of geniculo-cortical connectivity in area 17 of the cat. *Journal of Physiology* **342**, 181–215.

FREUND, T. F., MARTIN, K. A. C., SMITH, A. D. & SOMOGYI, P. (1983). Glutamate decarboxylase-immunoreactive terminals of Golgi-impregnated axo-axonic cells and of presumed basket cells in synaptic contact with pyramidal neurons of the cat's visual cortex. *Journal of Comparative Neurology* **221**, 263–278.

FREUND, T. F., MARTIN, K. A. C., SOMOGYI, P. & WHITTERIDGE, D. (1985*a*). Innervation of cat visual areas 17 and 18 by physiologically identified X- and Y-type thalamic afferents. II. Identification of postsynaptic targets by GABA immunocytochemistry and Golgi impregnation. *Journal of Comparative Neurology* **242**, 275–291.

FREUND, T. F., MARTIN, K. A. C. & WHITTERIDGE, D. (1985*b*). Innervation of cat visual areas 17 and 18 by physiologically identified X- and Y-type thalamic afferents. I. Arborization patterns and quantitative distribution of postsynaptic elements. *Journal of Comparative Neurology* **242**, 263–274.

GABBOTT, P. L. A., MARTIN, K. A. C. & WHITTERIDGE, D. (1987). The connections between pyramidal neurons in layer V of cat visual cortex (area 17). *Journal of Comparative Neurology* **259**, 364–381.

GABBOTT, P. L. A. & SOMOGYI, P. (1986). Quantitative distribution of GABA-immunoreactive neurons in the visual cortex (area 17) of the cat. *Experimental Brain Research* **61**, 323–331.

GANZ, L. & FELDER, R. (1984). Mechanism of directional selectivity in simple neurons of the cat's visual cortex analyzed with stationary flash sequences. *Journal of Neurophysiology* **51**, 294–324.

GETTING, P. A. (1989). Reconstruction of small neural networks. In *Methods in Neuronal Modelling: From Synapses to Networks*, ed. KOCH, C. & SEGEV, I., pp. 171–194. MIT Press/Bradford Books, Cambridge, MA, USA.

GILBERT, C. D. (1977). Laminar differences in receptive field properties of cells in cat primary visual cortex. *Journal of Physiology* **268**, 391–421.

GILBERT, C. D. & WIESEL, T. N. (1979). Morphology and intracortical projections of functionally characterised neurons in the cat visual cortex. *Nature* **280**, 120–125.

GOODWIN, A. W. & HENRY, G. H. (1975). Direction selectivity of complex cells in comparison with simple cells. *Journal of Neurophysiology* **38**, 1524–1540.

GOODWIN, A. W., HENRY, G. H. & BISHOP, P. O. (1975). Direction selectivity of simple striate cells: properties and mechanism. *Journal of Neurophysiology* **38**, 1500–1523.

HEGGELUND, P. (1981). Receptive field organization of simple cells in cat striate cortex. *Experimental Brain Research* **42**, 89–98.

HENRY, G. H., HARVEY, A. R. & LUND, J. S. (1979). The afferent connections and laminar distribution of cells in the cat striate cortex. *Journal of Comparative Neurology* **187**, 725–744.

HOFFMAN, K.-P. & STONE, J. (1971). Conduction velocity of afferents to cat visual cortex: A correlation with cortical receptive field properties. *Brain Research* **32**, 460–466.

HUBEL, D. H. & WIESEL, T. N. (1959). Receptive fields of single neurones in the cat's striate cortex. *Journal of Physiology* **148**, 574–591.

HUBEL, D. H. & WIESEL, T. N. (1962). Receptive fields, binocular interaction and functional architecture in the cat's visual cortex. *Journal of Physiology* **160**, 106–154.

HUMPHREY, A. L., SUR, M., UHLRICH, D. J. & SHERMAN, S. M. (1985). Projection patterns of individual X- and Y-cell axons from the lateral geniculate nucleus to cortical area 17 in the cat. *Journal of Comparative Neurology* **233**, 159–189.

JACK, J. J. B., NOBLE, D. & TSIEN, R. W. (1975). *Electric Current Flow in Excitable Cells*. Oxford University Press, Oxford.

KELLY, J. S. & KRNJEVIĆ, K. (1969). The action of glycine on cortical neurons. *Experimental Brain Research* **9**, 155–163.

KISVÁRDAY, Z. F., MARTIN, K. A. C., FREUND, T. F., MAGLOCSKY, Z. S., WHITTERIDGE, D. & SOMOGYI, P. (1986). Synaptic targets of HRP-filled layer III pyramidal cells in the cat striate cortex. *Experimental Brain Research* **64**, 541–552.

KISVÁRDAY, Z. F., MARTIN, K. A. C., FRIEDLANDER, M. J. & SOMOGYI, P. (1987). Evidence for interlaminar inhibitory circuits in striate cortex of cat. *Journal of Comparative Neurology* **260**, 1–19.

KISVÁRDAY, Z. F., MARTIN, K. A. C., WHITTERIDGE, D. & SOMOGYI, P. (1985). Synaptic connections of intracellularly filled clutch cells: a type of small basket cell in the visual cortex of the cat. *Journal of Comparative Neurology* **241**, 111–137.

KOCH, C., DOUGLAS, R. J. & WEHMEIER, U. (1990). Visibility of synaptically induced conductance changes: Theory and simulations of anatomically characterized cortical pyramidal cells. *Journal of Neuroscience* **10**, 1728–1744.

KOCH, C. & POGGIO, T. (1983). A theoretical analysis of the electrical properties of spines. *Proceedings of the Royal Society* B **218**, 455–477.

KOCH, C. & POGGIO, T. (1985*a*). The synaptic veto mechanism: does it underlie direction and orientation selectivity in the visual cortex? In *Models of the Visual Cortex*, ed. ROSE, D. R. & DOBSON, V. G., pp. 408–419. John Wiley & Sons, Chichester, New York.

KOCH, C. & POGGIO, T. (1985*b*). A simple algorithm for solving the cable equation in dendritic trees of arbitrary geometry. *Journal of Neuroscience Methods* **12**, 303–315.

LEVENTHAL, A. G. (1979). Evidence that the different classes of relay cells of the cat's lateral geniculate nucleus terminate in different layers of the striate cortex. *Experimental Brain Research* **37**, 349–372.

LI, CH.-L. & CHOU, S. N. (1962). Cortical intracellular synaptic potentials and direct cortical stimulation. *Journal of Cellular and Comparative Physiology* **60**, 1–16.

LI, CH.-L., ORTIZ-GALVIN, A., CHOU, S. N. & HOWARD, S. Y. (1960). Cortical intracellular potentials in response to stimulation of lateral geniculate body. *Journal of Neurophysiology* **23**, 592–601.

LUND, J. S., HENRY, G. H., MACQUEEN, C. L. & HARVEY, A. R. (1979). Anatomical organization of the primary visual cortex (area 17) of the cat. A comparison with area 17 of the macaque monkey. *Journal of Comparative Neurology* **184**, 599–618.

MCCORMICK, D. A., CONNORS, B. W., LIGHTHALL, J. W. & PRINCE, D. A. (1985). Comparative electrophysiology of pyramidal and sparsely spiny stellate neurons of the neocortex. *Journal of Neurophysiology* **54**, 782–806.

MCGUIRE, B. A., HORNUNG, J.-P., GILBERT, C. D. & WIESEL, T. N. (1984). Patterns of synaptic input to layer 4 of cat striate cortex. *Journal of Neuroscience* **4**, 3021–3033.

MARTIN, K. A. C. (1984). Neuronal circuits in cat striate cortex. In *Cerebral Cortex*, vol. 2. *Functional Properties of Cortical Cells*, ed JONES, E. G. & PETERS, A., pp. 241–284. Plenum Press, New York.

MARTIN, K. A. C. (1988). The Wellcome Prize Lecture. From single cells to simple circuits in the cerebral cortex. *Quarterly Journal of Experimental Physiology* **73**, 637–702.

MARTIN, K. A. C., FRIEDLANDER, M. J. & ALONES, V. (1989). Physiological, morphological, and cytochemical characteristics of a layer 1 neuron in cat striate cortex. *Journal of Comparative Neurology* **282**, 404–414.

MARTIN, K. A. C. & SOMOGYI, P. (1985). Local excitatory circuits in area 17. In *Models of the Visual Cortex*, ed. ROSE, D. R. & DOBSON, V. G., pp. 504–513. John Wiley & Sons, Chichester, New York.

MARTIN, K. A. C., SOMOGYI, P. & WHITTERIDGE, D. (1983). Physiological and morphological properties of identified basket cells in the cat's visual cortex. *Experimental Brain Research* **50**, 193–200.

MARTIN, K. A. C. & WHITTERIDGE, D. (1984). Form, function and intracortical projections of spiny neurones in the striate visual cortex of the cat. *Journal of Physiology* **353**, 463–504.

MEAD, C. A. (1989). *Analog VLSI and Neural Systems*. Addison–Wesley Publishing, Reading, MA, USA.

NEWBERRY, N. R. & NICOLL, R. A. (1985). Comparison of the action of baclofen with γ-aminobutyric acid on rat hippocampal pyramidal cells *in vitro*. *Journal of Physiology* **360**, 161–185.

ORBAN, G. A. (1984). *Neuronal Operations in the Visual Cortex*. Springer Verlag, Berlin, Heidelberg.

ORBAN, G. A., KENNEDY, H. & MAES, H. (1981). Response to movement of neurons in areas 17 and 18 of the cat: Direction selectivity. *Journal of Neurophysiology* **45**, 1059–1072.

PETERS, A. & REGIDOR, J. (1981). A reassessment of the forms of the nonpyramidal neurons in area 17 of cat visual cortex. *Journal of Comparative Neurology* **203**, 685–716.

RALL, W. (1977). Core conductor theory and cable properties of neurons. In *Handbook of Physiology* vol. 1, *The Nervous System*, ed. KANDEL, E. R., BROOKHARDT, J. M. & MOUNTCASTLE, V. B., pp. 39–98. Williams & Wilkins Co., Baltimore, MD, USA.

RALL, W. & RINZEL, J. (1973). Branch input resistance and steady attenuation for input to one branch of a dendritic neurone model. *Biophysical Journal* **13**, 648–688.

RAMÓN Y CAJAL, S. (1911). *Histologie du Système Nerveux de l'Homme et des Vertébrés*, vol. II, pp. 599–618. Maloine, Paris.

RINZEL, J. & RALL, W. (1974). Transient response in a dendritic neurone model for current injected at one branch. *Biophysical Journal* **14**, 759–790.

ROCKEL, A. J., HIORNS, R. W. & POWELL, T. P. S. (1980). The basic uniformity in structure of the neocortex. *Brain* **103**, 221–244.

SCHWINDT, P. C., SPAIN, W. J., FOEHRING, R. C., STAFSTROM, C. E., CHUBB, M. C. & CRILL, W. E. (1988*a*). Multiple potassium conductances and their functions in neurons from cat sensorimotor cortex *in vitro*. *Journal of Neurophysiology* **59**, 424–449.

SCHWINDT, P. C., SPAIN, W. J., FOEHRING, R. C., STAFSTROM, C. E., CHUBB, M. C. & CRILL, W. E. (1988*b*). Slow conductances in neurons from cat sensorimotor cortex *in vitro* and their role in slow excitability changes. *Journal of Neurophysiology* **59**, 450–467.

SILLITO, A. M. (1975). The contribution of inhibitory mechanisms to the receptive field properties of neurones in the striate cortex of the cat. *Journal of Physiology* **250**, 305–329.

SILLITO, A. M. (1979). Inhibitory mechanisms influencing complex cell orientation selectivity and their modification at high resting discharge levels. *Journal of Physiology* **289**, 33–53.

SOMOGYI, P. (1989). Synaptic organization of GABAergic neurons and $GABA_A$ receptors in the lateral geniculate nucleus and visual cortex. In *Neural Mechanisms of Visual Perception*, ed. LAM, D. K.-T. & GILBERT, C. D., pp. 35–62. Portfolio Publishing Co., Houston, TX, USA.

SOMOGYI, P., KISVÁRDAY, Z. F., MARTIN, K. A. C. & WHITTERIDGE, D. (1983). Synaptic connections of morphologically identified and physiologically characterized large basket cells in the striate cortex of cat. *Neuroscience* **10**, 261–294.

SOMOGYI, P. & MARTIN, K. A. C. (1985). The role of inhibitory interneurones in the function of area 17. In *Models of the Visual Cortex*, ed. ROSE, D. R. & DOBSON, V. G., pp. 514–523. John Wiley & Sons, Chichester, New York.

SOMOGYI, P. & SOLTÉSZ, I. (1986). Immunogold demonstration of GABA in synaptic terminals of intracellularly recorded, horseradish peroxidase-filled basket cells and clutch cells in the cat's visual cortex. *Neuroscience* **19**, 1051–1065.

TOYAMA, K., MATSUNAMI, K. & OHNO, T. (1969). Antidromic identification of association, commissural and corticofugal efferent cells in cat visual cortex. *Brain Research* **14**, 513–517.

TSUMOTO, T., ECKART, W. & CREUTZFELDT, O. D. (1979). Modification of orientation sensitivity of cat visual cortex neurons by removal of GABA-mediated inhibition. *Experimental Brain Research* **34**, 351–363.

WATANABE, S., KONISHI, M. & CREUTZFELDT, O. D. (1966). Postsynaptic potentials in the cat's visual cortex following electrical stimulation of the afferent pathways. *Experimental Brain Research* **1**, 272–283.

WEHMEIER, U., DONG, D., KOCH, C. & VAN ESSEN, D. (1989). Modeling the mammalian visual cortex. In *Methods in Neuronal Modeling: From Synapses to Networks*, ed. KOCH, C. & SEGEV, I., pp. 335–361. MIT Press/Bradford Books, Cambridge, MA, USA.

WHITE, E. L. (1989). *Cortical Circuits*. Birkhauser, Boston.

WINFIELD, D. A., GATTER, K. C. & POWELL, T. P. S. (1980). An electron microscopic study of the types and proportions of neurons in the motor cortex and visual areas of the cat and rat. *Brain* **103**, 245–258.